

Discovery of Potent and Selective Inhibitors of Cdc2-Like Kinase 1 (CLK1) as a New Class of Autophagy Inducers

Qi-Zheng Sun,^{†,‡} Gui-Feng Lin,^{†,‡} Lin-Li Li,^{‡,§} Xi-Ting Jin,[‡] Lu-Yi Huang,^{†,§} Guo Zhang,[‡] Wei Yang,[‡] Kai Chen,[†] Rong Xiang,^{||} Chong Chen,[†] Yu-Quan Wei,[†] Guang-Wen Lu,^{*,†,§} and Sheng-Yong Yang^{*,†,§,¶}

[†]State Key Laboratory of Biotherapy and Cancer Center, West China Hospital, Sichuan University and Collaborative Innovation Center for Biotherapy, Chengdu 610041, P.R. China

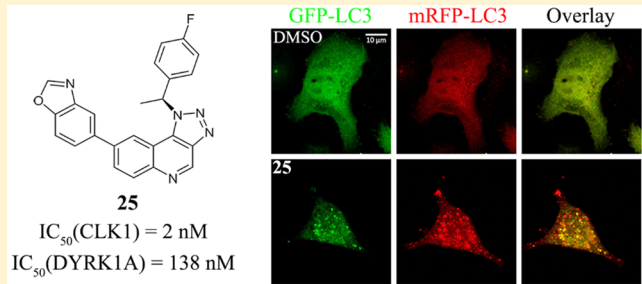
[‡]Key Laboratory of Drug Targeting and Drug Delivery System of Ministry of Education, West China School of Pharmacy, Sichuan University, Sichuan 610041, P.R. China

[§]School of Chemical Engineering, Sichuan University and Collaborative Innovation Center for Biotherapy, Chengdu 610041, P.R. China

^{||}Department of Clinical Medicine, School of Medicine, Nankai University, Tianjin 300071, P.R. China

Supporting Information

ABSTRACT: Autophagy inducers represent new promising agents for the treatment of a wide range of medical illnesses. However, safe autophagy inducers for clinical applications are lacking. Inhibition of cdc2-like kinase 1 (CLK1) was recently found to efficiently induce autophagy. Unfortunately, most of the known CLK1 inhibitors have unsatisfactory selectivity. Herein, we report the discovery of a series of new CLK1 inhibitors containing the 1*H*-[1,2,3]triazolo[4,5-*c*]quinoline scaffold. Among them, compound 25 was the most potent and selective, with an IC₅₀ value of 2 nM against CLK1. The crystal structure of CLK1 complexed with compound 25 was solved, and the potency and kinase selectivity of compound 25 were interpreted. Compound 25 was able to induce autophagy in *in vitro* assays and displayed significant hepatoprotective effects in the acetaminophen (APAP)-induced liver injury mouse model. Collectively, due to its potency and selectivity, compound 25 could be used as a chemical probe or agent in future mechanism-of-action or autophagy-related disease therapy studies.



1. INTRODUCTION

Autophagy is a type of cell “self-eating” phenomenon that can selectively remove damaged or useless organelles and proteins, thus protecting cells from death. Impaired autophagic activity has been linked to a wide range of diseases, including cancer,¹ diabetes,^{2,3} neurodegenerative diseases,^{4,5} and drug-induced organ injury.^{6,7} Autophagy inducers are thus thought of as promising agents for the treatment of these diseases.⁸ Currently, only a few autophagy inducers are known.⁹ Nevertheless, most of these agents have a wide range of pharmacological activity, which implies a potential risk of toxicity, thus restricting their clinical application.¹⁰ For example, rapamycin, a typical autophagy inducer, could depress the immune system^{11,12} and induce insulin resistance.^{13,14} Therefore, there is an urgent need to discover more efficient and specific autophagy inducers.

In a recent study, Fant et al.¹⁵ demonstrated that inhibition of cdc2-like kinase 1 (CLK1) could efficiently induce autophagy. The authors also indicated that CLK1 could be a target for the treatment of autophagy-related diseases. To date, a number of CLK1 inhibitors have been reported.^{16–21} Despite few inhibitors with definite selectivity, most of the reported

CLK1 inhibitors belong to the miscellaneous type, which are associated with unsatisfactory kinase selectivity and are thus not suitable for clinical use due to possible side effects. In particular, these inhibitors, without exception, displayed identical or similar potency against CLK1 and dual-specificity tyrosine-phosphorylation-regulated kinase 1A (DYRK1A).^{18,22} DYRK1A is highly homologous in sequence to CLK1,¹⁸ and inhibition of DYRK1A has been shown to pose a potential toxicological risk.^{23,24} Therefore, the identification of potent and selective CLK1 inhibitors may have potential clinical application value in the treatment of autophagy-related diseases.

In the effort to seek potent and selective CLK1 inhibitors, we recently obtained a hit compound, 1-methyl-8-(2-methylpyridin-4-yl)-1*H*-[1,2,3]triazolo[4,5-*c*]quinoline (1, Figure 1) (for details, see Supporting Information). Compound 1 showed IC₅₀ values of 139 and 420 nM against CLK1 and DYRK1A, respectively. Both the activity and selectivity of this compound were poor and required further optimization. The main purpose of this investigation was to carry out structural

Received: May 4, 2017

Published: July 10, 2017

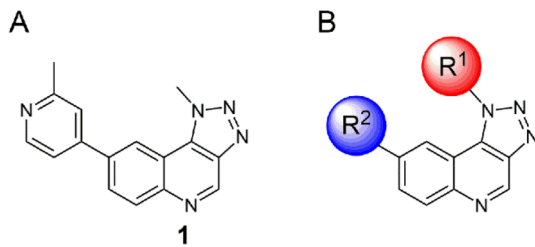


Figure 1. (A) Chemical structure of compound 1. (B) Regions of focus for structural optimization.

optimization and structure–activity relationship (SAR) analyses of compound 1. We further explored the ability of the most active and selective compound to induce autophagy and explored possible hepatoprotective effects in the acetaminophen (APAP)-induced acute liver injury mouse model.

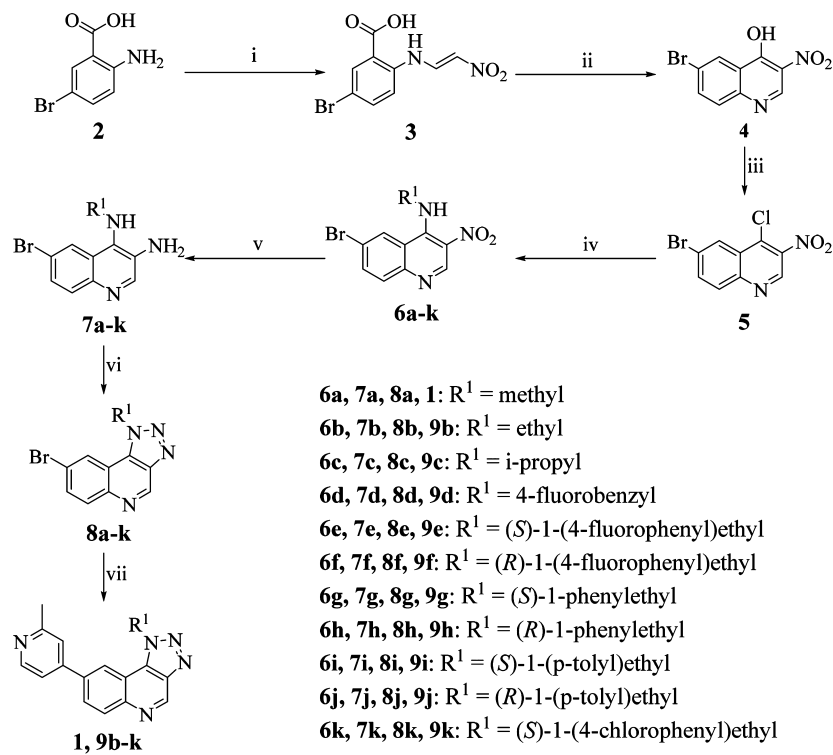
2. RESULTS AND DISCUSSION

2.1. Chemical Syntheses and SAR Analyses. The subsequent structural optimization was focused on the R¹ and R² regions of 1 (Figure 1B). In the first step, we fixed R² as the original 2-methylpyridin-4-yl group and varied the R¹ group substituents. The synthetic routes are outlined in Scheme 1. Briefly, commercially available 2 was reacted with self-prepared 2-nitroacetaldehyde oxime to obtain 3, which was dehydrated to yield 4. Chlorination of 4 afforded the key intermediate 5. A nucleophilic substitution reaction between 5 and various substituted amines yielded intermediates 6a–6k. The nitro groups of 6a–6k were reduced to produce the corresponding amines 7a–7k, which then underwent a diazotization and

condensation reaction to produce the triazole compounds 8a–8k. Final product compounds 1 and 9b–9k were readily obtained through the classic palladium-catalyzed Suzuki coupling between 8a–8k and (2-methylpyridin-4-yl)boronic acid (29).

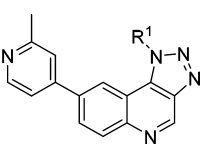
The chemical structures and bioactivities of 9b–9k and 1 are shown in Table 1. Here, a typical CLK1 inhibitor, (Z)-1-(3-ethyl-5-methoxybenzo[d]thiazol-2(3H)-ylidene)propan-2-one (30, called TG003 in literature),²⁵ was used as a positive control. In addition, we used the ratio of activities against DYRK1A and CLK1 as a selectivity index (SI) to represent the selectivity of compounds, which was primarily based on the following considerations. First, the systematic evaluation of the kinase selectivity must assess the activity of compounds against the entire kinase, which is extremely costly. Second, the amino acid sequences of DYRK1A and CLK1 are very similar, with an identity of 70.4%, and the majority of CLK1 inhibitors have comparable potency against DYRK1A. Table 1 shows that the introduction of a benzyl group at the R¹ position benefits the CLK1 activity (9d vs 1, 9b, and 9c). Methylation at the benzylic carbon atom leads to chiral derivatives, and the S-configuration is more favorable for selectivity (9e vs 9f, 9g vs 9h). In addition, the C4 substitution on the phenyl group is sensitive to both potency and selectivity. Compared with the unsubstituted 9g, compound 9e with a fluorine (–F) substitution showed the most selectivity, although its potency was marginally decreased. Other substituents, including –methyl (9i) and –Cl (9k) groups, decreased both the activity and selectivity. To summarize, 9e, which contains a (S)-1-(4-fluorophenyl)ethyl group at the R¹ position, had the highest selectivity and also considerable potency against CLK1.

Scheme 1. Synthetic Routes of 1 and 9b–9k^a



^aReagents and conditions: (i) (1) HCl, H₂O, room temperature (rt), (2) NaOH, H₂O, 0 °C, (3) HCl, H₂O, 0 °C; (ii) AcOK, Ac₂O, 120 °C; (iii) POCl₃, reflux; (iv) substituted amine, triethylamine, EtOH, reflux; (v) Fe, HAc, 60 °C; (vi) NaNO₂, AcOH/H₂O; (vii) 29, Pd(dppf)Cl₂, K₂CO₃, 1,4-dioxane/H₂O, 100 °C, 24 h.

Table 1. Structures and Bioactivities (IC_{50}) of Compounds 9b–k and 1^a



Cpd.	R ¹	CLK1 [nM]	DYRK1A [nM]	SI ^b
1	—	139	420	3
9b	—	66	283	4
9c	—	64	404	6
9d		7	107	15
9e		29	1303	45
9f		36	194	5
9g		6	177	30
9h		24	245	10
9i		173	1337	8
9j		34	141	4
9k		155	1756	11
30 ^c		17	71	4

^a IC_{50} values were determined using the KinaseProfiler from Eurofins. The data represent the mean values of two independent experiments.

^bSI denotes the ratio of IC_{50} (DYRK1A) to IC_{50} (CLK1). ^cpositive control; [ATP] = 10 μ M.

In the second step, we fixed R¹ as the optimal (S)-1-(4-fluorophenyl)ethyl group and altered the R² group using different subgroups, including phenyl, pyridyl, substituted phenyl and pyridyl, morpholinyl, five-membered heterocyclic rings, and benzo-fused five-membered heterocyclic rings. Another 16 new compounds (10–25) were then synthesized.

The synthetic routes to these compounds are depicted in Scheme 2. Briefly, Suzuki coupling of 8e with commercially available aromatic boric acid (or ester) yielded products 10–15 and 17–24, and palladium-catalyzed Buchwald coupling between morpholine and 8e produced product 16. By refluxing commercially available 2-amino-4-bromophenol (26) in triethyl orthoformate, 5-bromobenzo[d]oxazole (27) could be readily obtained, which subsequently underwent a Miyaura borylation reaction to yield a benzooxazole-5-boronic acid pinacol ester

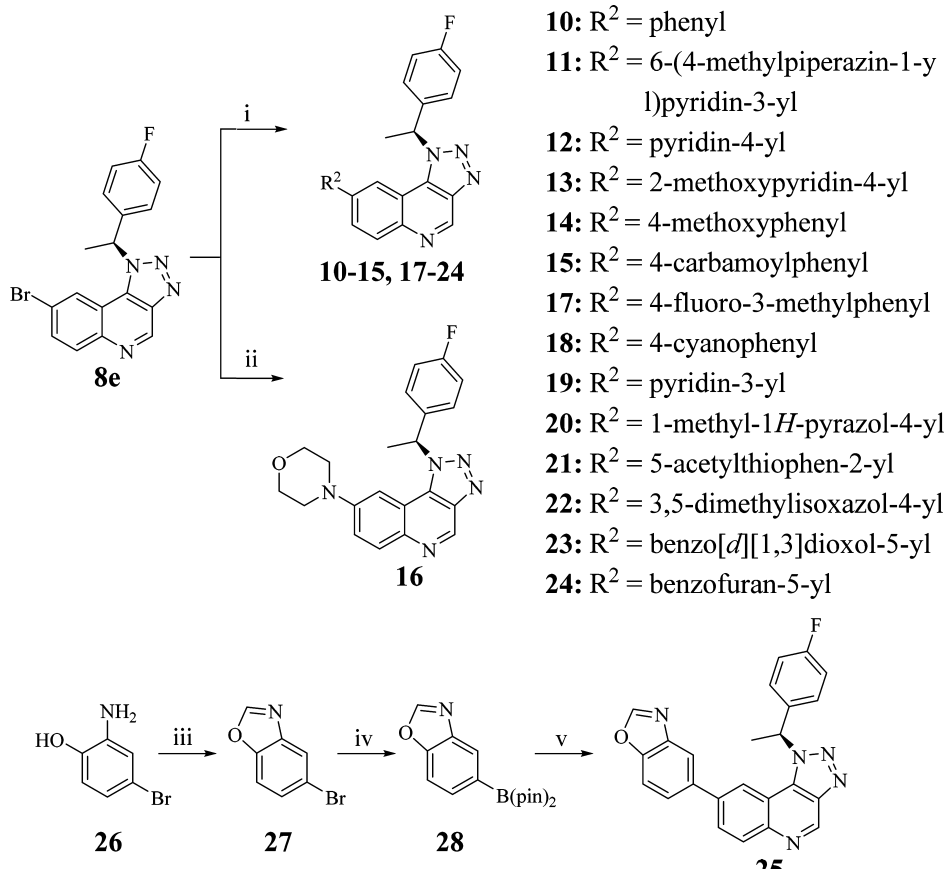
(28). Then, Suzuki coupling of 28 with 8e yielded the final product 25.

The chemical structures and bioactivities of compounds 10–25 are shown in Table 2, revealing that substitutions at the R² position substantially impacted the activity and selectivity. Compared with 9e, compounds with bromo (8e), phenyl (10), substituted phenyl (14, 15, 17, and 18), pyridyl (12, 19), substituted pyridyl (11, 13), morpholinyl (16), or five-membered heterocyclic (20–22) groups at the R² position had significantly decreased or completely absent CLK1 activities. Compounds (23–25) containing a benzo-fused five-membered heterocyclic group at the R² position seemed to have overall improved activity and selectivity. Among them, compound 25 with a benzo[d]oxazol-5-yl moiety at the R² position exhibited the best performance, with an IC_{50} value of 2 nM against CLK1 and 69-fold increased potent activity compared with that of the closely related kinase DYRK1A.

Collectively, compound 25, which contained (S)-1-(4-fluorophenyl)ethyl and benzo[d]oxazol-5-yl groups at the R¹ and R² positions, respectively, showed the highest potency and selectivity in enzymatic assays. Further in-depth studies were then performed on this compound, including measurement of kinase-wide selectivity, cocrystal structure determination, in vitro autophagy-inducing ability examination, and assessment of the in vivo effect of liver protection in an acute liver injury model.

2.2. Kinome-wide Selectivity of 25. The selectivity of the compounds described above were only for DYRK1A. To examine the kinase-wide selectivity of 25, we tested the kinase inhibition profiles of this compound against a panel of 357 recombinant human protein kinases. The inhibitory activities of 25 at a fixed concentration of 10 μ M were measured first. For kinases with inhibitory rates higher than 50%, further IC_{50} values were determined. The results are presented in Supporting Information, Table S1. A dendrogram representation of the kinase inhibition by 25 is also shown in Supporting Information, Figure S2. As expected, CLK1 was the most potently inhibited kinase (IC_{50} : 2 nM). In addition to CLK1, only two kinases had an IC_{50} value less than 100 nM, namely CLK2 (IC_{50} : 31 nM) and CLK4 (IC_{50} : 8 nM), which are isoforms of CLK1. Except for the CLks, DYRK1A was the strongest off-target. Furthermore, Supporting Information, Table S1 shows that 25 displayed at least 110-fold selectivity toward CLK1 over 351 of the 357 kinases tested (98.32%). Of note is that compound 25 did not show obvious activity against 292 kinases ($IC_{50} > 10 \mu$ M). To the best of our knowledge, 25 is the most potent and selective CLK1 inhibitor identified to date.

2.3. Co-crystal Structure of CLK1 Complexed with 25 and the Rationale for Its Potency and Selectivity. To elucidate the interactions between 25 and CLK1 and the molecular basis of the observed kinase selectivity, we solved the cocrystal structure of the CLK1 kinase domain with 25 at a resolution of 1.9 \AA (PDB 5X8I). The related data processing and structure refinement statistics are provided in Supporting Information, Table S2. Figure 2A displays the key interactions of 25 with CLK1, illustrating that 25 suitably resides in the ATP binding pocket of CLK1, with the benzo[d]oxazol-5-yl group pointing toward the hinge region and the triazole moiety of the 1*H*-[1,2,3]triazolo[4,5-*c*]quinoline scaffold pointing toward the solvent area. The quinoline nitrogen and the kinase Lys191 forms an important hydrogen bond. Another important hydrogen bond is formed between the oxazole oxygen atom

Scheme 2. Synthetic Routes to 10–25^a

^aReagents and conditions: (i) commercially available aromatic boronic acid or boronic acid ester, Pd(dppf)Cl₂, K₂CO₃, 1,4-dioxane/H₂O, 100 °C, 24 h; (ii) morpholine, Pd₂(dba)₃, X-Phos, K₂CO₃, t-BuOH, 100 °C, overnight; (iii) triethyl orthoformate, reflux; (iv) bis(pinacolato)diboron, Pd(dppf)Cl₂, AcOK, 1,4-dioxane, 100 °C; (v) 8e, Pd(dppf)Cl₂, K₂CO₃, 1,4-dioxane/H₂O, 100 °C, 24 h.

and Leu244 on the hinge, with the oxazole oxygen atom acting as a hydrogen bond acceptor. The oxazole nitrogen might form some interactions with the hinge region through a water-mediated hydrogen-bond network, which might partially explain the potency increase of benzoxazole **25** compared to benzofuran **24**. In addition, it was also obvious that the tricyclic scaffold of **25** formed a T-shape π – π interaction with the benzene ring of CLK1 Phe241 and a π – π stacking interaction with the benzene ring of Phe172. Here, it is worth mentioning that quinoline-containing kinase inhibitors usually adopt a canonical hinge binding mode with quinoline making the hinge contacts in the ATP-binding pocket of kinase.^{26–28} However, in this case, **25**, which also contains quinoline, adopts an unusual binding mode. Thus, some important interactions indicated above are formed, which could be one of the reasons why the inhibitor shows such a good selectivity.

To understand the preference of **25** in the inhibition of CLK1 over other kinases, the active amino acids involved in CLK1/**25** interactions were compared between different kinases via sequence alignment. Figure 2B shows the alignment of the key residues within 4.5 Å of **25** and CLK1 with the corresponding residues of other selected kinases (note that numbering is according to CLK1) that include CLK1–4, DYRK isoforms, and other representative kinases inhibited by **25**, with IC₅₀ values of different orders of magnitude. Obviously, the potencies of **25** against different kinases were strongly dependent on the residues in their active pockets.

CLK2/4 had the same residues as CLK1 in the alignment, explaining why they were potently inhibited by **25**. The main difference between CLK1/2/4 and CLK3 is the residue 324 (CLK1, valine; CLK3, alanine). We noted that alanine had a smaller hydrophobic side chain compared with valine and thus likely weakened the hydrophobic interactions with the ligand. We hypothesize that this may be the reason why **25** had reduced activity against CLK3. Similarly, DRYK1A and DRYK1B displayed moderate activity. In sequence, these two kinases had one residue that differed from CLK1 (CLK1, LEU167, vs DRYK1A/1B, ILE167). Notably, the substitution of LEU167 (as in CLK1) with ILE167 (as in DRYK1A/1B) created small amounts of steric hindrance with **25**, thus requiring a possible conformational adjustment in the residue to properly accommodate the bound ligand. Accordingly, **25** exhibited decreased activity against DRYK1A/B compared with CLK1. Finally, other selected kinases all exhibit more profound residue differences in the ligand binding site, explaining the poor activities of **25** against these proteins.

2.4. Effects of 25 on the Subcellular Redistribution of Downstream Serine/Arginine-Rich (SR) Proteins in Intact Cells. SR proteins are typical downstream substrates of CLK1. It has been demonstrated that activation of CLks could induce redistribution of SR proteins from nuclear speckles (stored form) to the nucleoplasm (active form).^{29,30} Therefore, to examine whether **25** can inhibit CLK1 activation in intact cells, we measured the distribution of SR proteins in

Table 2. Structures and Bioactivities (IC_{50}) of Compounds 10–25^a

Cpd.	R ₂	CLK1 [nM]	DYRK1A [nM]	SI ^b
9e		29	1303	45
8e	Br	>10000	>10000	-
10		4985	>10000	2
11		>10000	>10000	-
12		189	1139	6
13		430	2872	7
14		439	>10000	23
15		186	>10000	54
16		529	3360	6
17		>10000	>10000	-
18		>10000	>10000	-
19		>10000	>10000	-
20		280	3356	12
21		993	>10000	10
22		>10000	>10000	-
23		18	257	14
24		30	1318	44
25		2	138	69
30 ^c	-	17	71	4

^a IC_{50} values were determined using the KinaseProfiler of Eurofins. The data represent the mean values of two independent experiments.
^bSI denotes the ratio of IC_{50} (DYRK1A) to IC_{50} (CLK1). ^cPositive control; [ATP] = 10 μ M.

cells by immunofluorescence before and after **25** treatment. Here, BNL CL.2 (mouse embryonic liver cell line) was

selected, and three concentrations (20 nM, 100 nM, and 10 μ M) of **25** were used. As shown in Figure 3 and Supporting Information, Figure S4, **25** treatment indeed led to the redistribution of SR proteins from the nucleoplasm to nuclear speckles, and the potency showed significant dose dependency. The same effect was observed for the positive control **30**. From here, we concluded that **25** could efficiently inhibit the activation of CLK1 in intact cells.

2.5. Ability of **25 to Induce Autophagy in Vitro.** We next examined the ability of **25** to induce autophagy in BNL CL.2 and SKOV-3 (human ovarian cancer cell line) cells. Compound **30** and the classic autophagy inducer rapamycin were used as positive controls. Western blot assays showed that **25** elevated the expression level of LC3II protein (a marker of autophagosomes^{31,32}) as well as the ratio of LC3II to LC3I (a sensitive index of autophagy^{33,34}) in a dose-dependent (Figures 4A and 5A) and time-dependent manner (Figure 4B). In accordance with the results of immunoblot assays, confocal microscopy examination showed that **25** increased the number of yellow LC3 puncta (colocalization of GFP and mRFP signals³⁵) in SKOV-3 cells infected with Ad-mRFP-GFP-LC3 (adenovirus-coding tandem GFP-mRFP-LC3), further confirming the formation of autophagosomes. The effects of **25** on yellow LC3 puncta also displayed obvious dose dependency, and a dose of 10 μ M showed the best performance (Figure 5B and Supporting Information, Figure S5). In addition, in **25**-treated cells, the number of red LC3 puncta (mRFP signals only³⁵) increased compared with that of DMSO-treated cells, indicating the formation of autolysosomes. Importantly, **25** stimulated the degradation of SQSTM1/p62 (a marker of autolysosomes³⁶ Figures 4A and 5A) and increased the ratio of red LC3 puncta to yellow LC3 puncta (Figure 5B and Supporting Information, Figure S5), both of which indicated an induction of autophagic flux by **25**. All of these data demonstrated that **25** could increase the synthesis and clearance of autophagosomes and induce autophagy and autophagic flux in vitro to levels higher than those resulting from **30** and rapamycin-induced autophagy, especially in BNL CL.2 cells. In contrast, compound **18** (negative control), which is inactive against CLK1 ($IC_{50} > 10 \mu$ M), could not trigger autophagy even at a concentration of 10 μ M (Supporting Information, Figure S6).

2.6. Protective Effect of **25 on APAP-Induced Acute Liver Injury.** As mentioned above, autophagy inducers may have potential applications in the treatment of relevant diseases. Drug-induced liver injury (DILI) is a major public health concern³⁷ and accounts for more than 50% of acute liver failure cases. APAP is a widely used antipyretic analgesic drug. However, an overdose of APAP can cause liver injury and even liver failure in humans³⁸ and is the most frequent cause of acute liver failure, especially in many western countries.³⁹ Ni et al.⁶ found that induction of autophagy by rapamycin inhibited APAP-induced hepatotoxicity, which restricted the necrotic areas and promoted liver regeneration and recovery.^{39,40} Herein, the APAP-induced hepatotoxicity mouse model was used to examine the therapeutic effect of **25** in vivo. As depicted in Figure 6A, APAP exposure resulted in severe liver injury, and treatment with **25** (ip, 30 mg/kg) imparted a significant hepatoprotective effect. We further detected the levels of the liver enzymes alanine aminotransferase (ALT) and aspartate aminotransferase (AST), high levels of which are considered to be indicators of liver damage. The results showed that treatment with **25** decreased serum ALT and AST levels

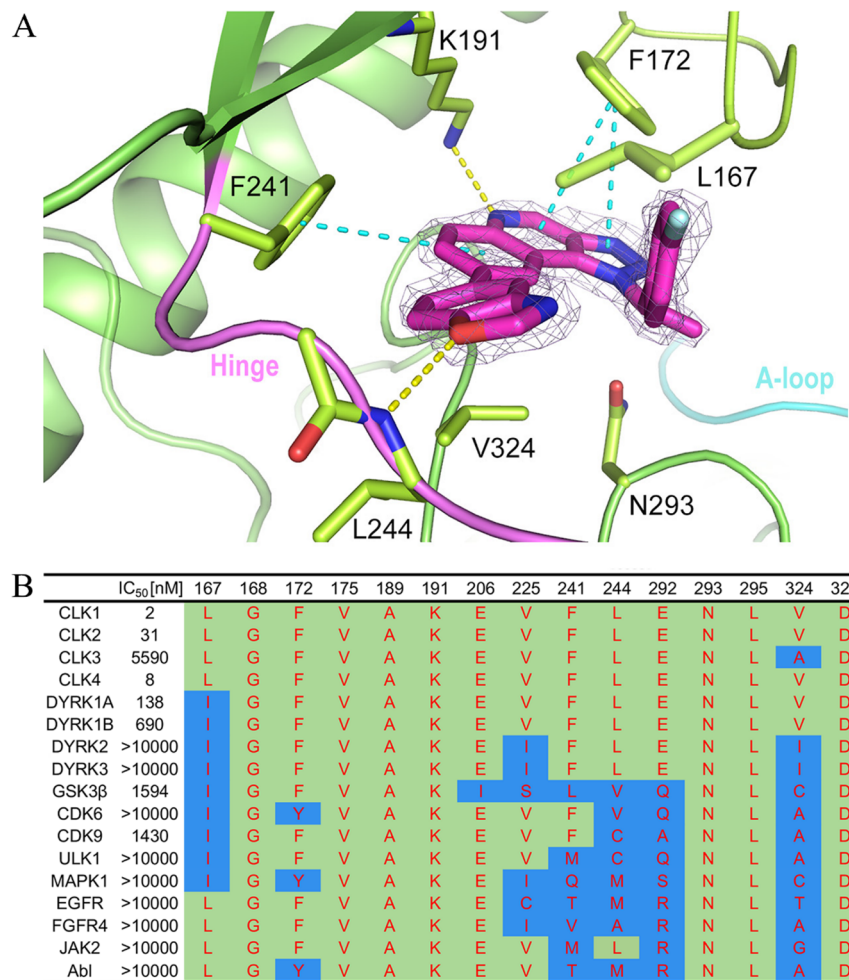


Figure 2. X-ray crystal structure of CLK1 complexed with **25** (PDB 5X8I). (A) Key interactions of **25** with the kinase active site. Yellow and cyan dashed lines indicate hydrogen bonds and $\pi-\pi$ interactions, respectively. Gray mesh: 2Fo–Fc omitted electron density map contoured at 2.0 σ . The images were produced using PyMOL. (B) Multiple-sequence alignment of the selected key residues within the ATP-binding pocket. The residues differing from the corresponding residues of CLK1 are highlighted in blue. Numbering is according to CLK1.

significantly such that both marker enzymes returned to normal levels (Figure 6B). Rapamycin and **30** also showed similar hepatoprotective effects in the same model.

3. CONCLUSIONS

In summary, a structural optimization of hit compound **1** led to the discovery of a series of new CLK1 inhibitors containing the scaffold 1*H*-[1,2,3]triazolo[4,5-*c*]quinolone. Among them, compound **25** is the most potent and selective. The co-crystal structure of **25** with CLK1 explained its potent activity and kinase selectivity. This compound also demonstrated an ability to induce autophagy *in vitro* and had significant hepatoprotective effects in the APAP-induced liver injury mouse model. A preliminary pharmacokinetic study in rats showed that **25** had good bioavailability (*F* = 52.86%, for more information see Supporting Information, Figure S7). All of these results imply that **25** could be a promising lead compound for the treatment of autophagy-related diseases. However, the mechanism by which CLK1 inhibition induces autophagy is currently unknown. Further studies, including an investigation of the mechanism of autophagy induction and preclinical evaluation in the treatment of autophagy-related diseases, are still underway in our laboratory.

4. EXPERIMENTAL SECTION

4.1. Chemistry Methods. All reagents and solvents were obtained from commercial suppliers and used without further purification unless otherwise indicated. Anhydrous solvents were dried and purified by conventional methods prior to use. Column chromatography was carried out on silica gel (300–400 mesh). All reactions were monitored by thin-layer chromatography (TLC), and silica gel plates with fluorescence F-254 were used and visualized with UV light. All of the final compounds were purified to >95% purity, as determined by high-performance liquid chromatography (HPLC). HPLC purity analysis was performed on a Waters 2695 HPLC system with the use of a Gemini C18 reversed-phase column (4.6 mm Φ \times 150 mm, particle size 5 μ m). The enantiomeric excess (ee) of the products was determined by HPLC analysis on Waters 2695 system using a Daicel Chiralpak IE chiral column (lot no. IE00CE-TG01S; part no. 8532S; particle size 5 μ m; dimensions 4.6 mm Φ \times 150 mm). Optical rotations were measured on a Rudolph Autopol VI automatic polarimeter, with $[\alpha]_D^{25}$ values reported in degrees and concentration (*c*) reported in g/100 mL. ^1H NMR and ^{13}C NMR spectra were recorded on a Bruker AV-400 spectrometer at 400 and 100 MHz, respectively. Coupling constants (*J*) are expressed in hertz (Hz). Spin multiplicities are described as s (singlet), d (doublet), t (triplet), dd (doublet of doublet), dt (doublet of triplet), q (quartet), quint (quintet), brs (broad singlet), and m (multiplet). Chemical shifts (δ) are listed in parts per million (ppm) relative to tetramethylsilane (TMS) as an internal standard. For ^{19}F NMR, chemical shifts are

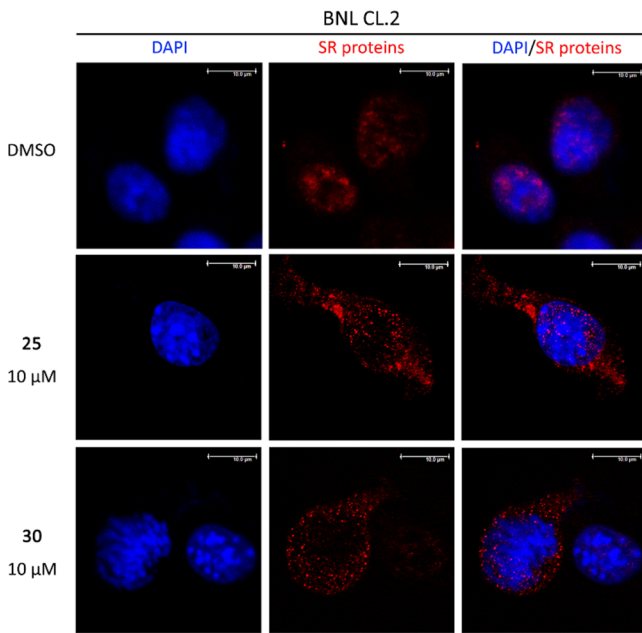


Figure 3. Compound **25** altered the location and redistribution of SR proteins. BNL CL.2 cells treated with **25** (10 μ M), **30** (10 μ M), or DMSO (0.1%) for 24 h were fixed and probed with anti-SR proteins antibody (mAb1H4G7). Diffuse staining and typical speckles demonstrated by mAb1H4G7 represent active and stored forms of SR proteins, respectively. DAPI was used to dye the nucleus. Scale bar: 10 μ m.

reported on a scale relative to CF₃COOH (δ -76.55 ppm in DMSO) as an external reference. Low-resolution and high-resolution ESI-MS readings were recorded on an Agilent 1200-G6410A mass spectrometer.

4.1.1. 1-Methyl-8-(2-methylpyridin-4-yl)-1*H*-[1,2,3]triazolo[4,5-*c*]quinolone (1). Compound **8a** (55 mg, 209.05 μ mol, 1 equiv), **29** (28.63 mg, 209.05 μ mol, 1 equiv), Pd(dppf)Cl₂ (15.3 mg, 20.9 μ mol, 0.1 equiv), and K₂CO₃ (86.67 mg, 627.14 μ mol, 3 equiv) were suspended in a mixed solution of 1,4-dioxane and water (4:1). Under a nitrogen atmosphere, the mixture was stirred at 100 °C for 24 h. The solvent was evaporated to dryness under reduced pressure to obtain

the crude product, which was purified by flash column chromatography to yield the desired product as a white powder (37.4 mg, 43% yield). ¹H NMR (400 MHz, DMSO-*d*₆) δ 9.58 (s, 1H), 8.81 (d, *J* = 1.8 Hz, 1H), 8.61 (d, *J* = 5.2 Hz, 1H), 8.37 (d, *J* = 8.7 Hz, 1H), 8.29 (dd, *J* = 8.7, 1.9 Hz, 1H), 7.86 (s, 1H), 7.79 (dd, *J* = 5.2, 1.5 Hz, 1H), 4.84 (s, 3H), 2.61 (s, 3H). ¹³C NMR (101 MHz, DMSO-*d*₆) δ 159.28, 150.17, 146.79, 145.77, 145.36, 141.16, 136.93, 133.70, 131.21, 128.72, 121.61, 121.58, 119.59, 116.32, 38.10, 24.70. ESI-MS *m/z* 276.2 [M + H]⁺.

4.1.2. (E)-5-Bromo-2-((2-nitrovinyl)amino)benzoic Acid (3). A suspension of 2-amino-5-bromo-benzoic acid (25 g, 115.72 mmol, 1 equiv) in 10:1 H₂O/HCl was stirred for 8 h and then filtered (solution A). Nitromethane (8.17 g, 133.85 mmol, 1.15 equiv) was added over 10 min to an ice bath-cooled mixture of ice (35 g) and NaOH (15.3 g, 382.53 mmol, 3.30 equiv). After stirring for 1 h at 0 °C and 1 h at rt, the solution was added to an ice-bath cooled mixture of ice (28 g) and HCl (37%, 42 mL) (solution B). Solutions A and B were combined, and the reaction mixture was stirred overnight at rt. The yellow precipitate was filtered off, washed with H₂O, and dried in vacuo to yield the crude product, which was used directly in the next step.

4.1.3. 6-Bromo-3-nitroquinolin-4-ol (4). Compound **3** (5 g, 17.42 mmol, 1 equiv) and potassium acetate (2.05 g, 20.90 mmol, 1.2 equiv) in acetic anhydride were stirred for 2 h at 120 °C. The precipitate was filtered and washed with acetic acid until the filtrate was colorless. The precipitate was further washed with water and then dried to obtain the title compound (2.32 g, two-step yield, 14%). ¹H NMR (400 MHz, DMSO-*d*₆) δ 13.21 (s, 1H), 9.24 (s, 1H), 8.32 (d, *J* = 2.3 Hz, 1H), 7.96 (dd, *J* = 8.8, 2.3 Hz, 1H), 7.71 (d, *J* = 8.8 Hz, 1H). ESI-MS *m/z*: 268.9 [M + H]⁺.

4.1.4. 6-Bromo-4-chloro-3-nitroquinoline (5). Compound **4** (2 g, 7.43 mmol) and POCl₃ were stirred for 4 h at 100 °C. The mixture was cooled to rt and slowly quenched with ice water. After neutralization with NaHCO₃ (aq), the aqueous phase was extracted with ethyl acetate and dried over Na₂SO₄. The product was obtained by evaporation of solution to dryness as a brown solid (2.1 g, 98% yield), which was used directly in the next step.

4.1.5. 6-Bromo-N-methyl-3-nitroquinolin-4-amine (6a). To a solution of **5** (1 g, 3.48 mmol, 1 equiv) and triethylamine (703.96 mg, 6.96 mmol, 2 equiv) in EtOH, methanamine hydrochloride (234.84 mg, 3.48 mmol, 1 equiv) was added slowly at rt. The resulting mixture was stirred at 60 °C for 4 h. The solution was concentrated in vacuo and then poured into water. The precipitate was filtered off and dried to obtain the desired product as a pale-yellow powder in 89% yield. ¹H NMR (400 MHz, DMSO-*d*₆) δ 8.94 (s, 1H), 8.89 (s, 1H), 8.67 (d, *J* = 1.4 Hz, 1H), 7.91 (dd, *J* = 8.8, 1.7 Hz, 1H), 7.78 (d, *J* = 8.8

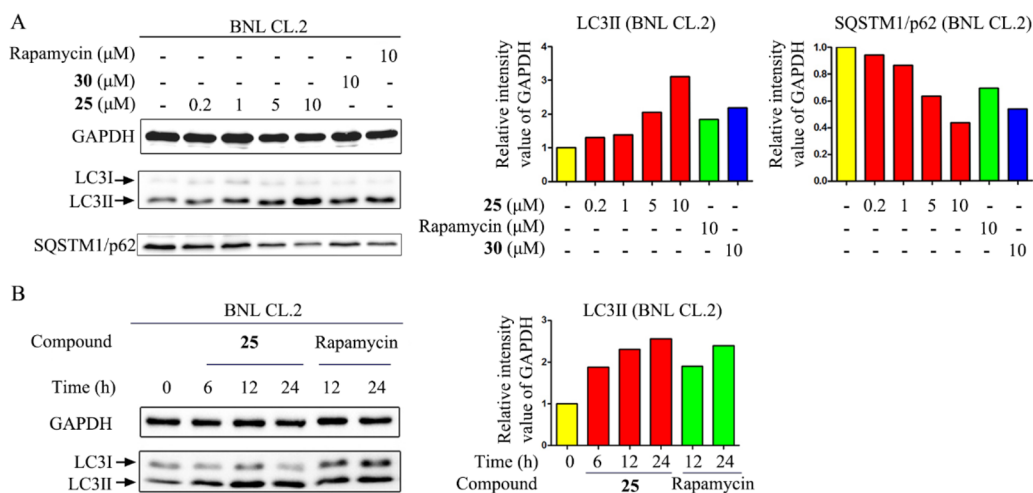


Figure 4. Detection of autophagy and autophagic flux induced by **25** in BNL CL.2 cells. (A) BNL CL.2 cells were treated with rapamycin (positive control), **30** (positive control), and various concentrations of **25** (0.2, 1, 5, and 10 μ M) for 24 h. Then, whole cell lysates were subjected to immunoblot assay to detect LC3 and SQSTM1/p62. Quantification of immunoblots is presented in the right panel. (B) BNL CL.2 cells were treated with **25** or rapamycin, and the level of LC3II protein was detected after 6, 12, and 24 h. Quantification of immunoblots is presented in the right panel.

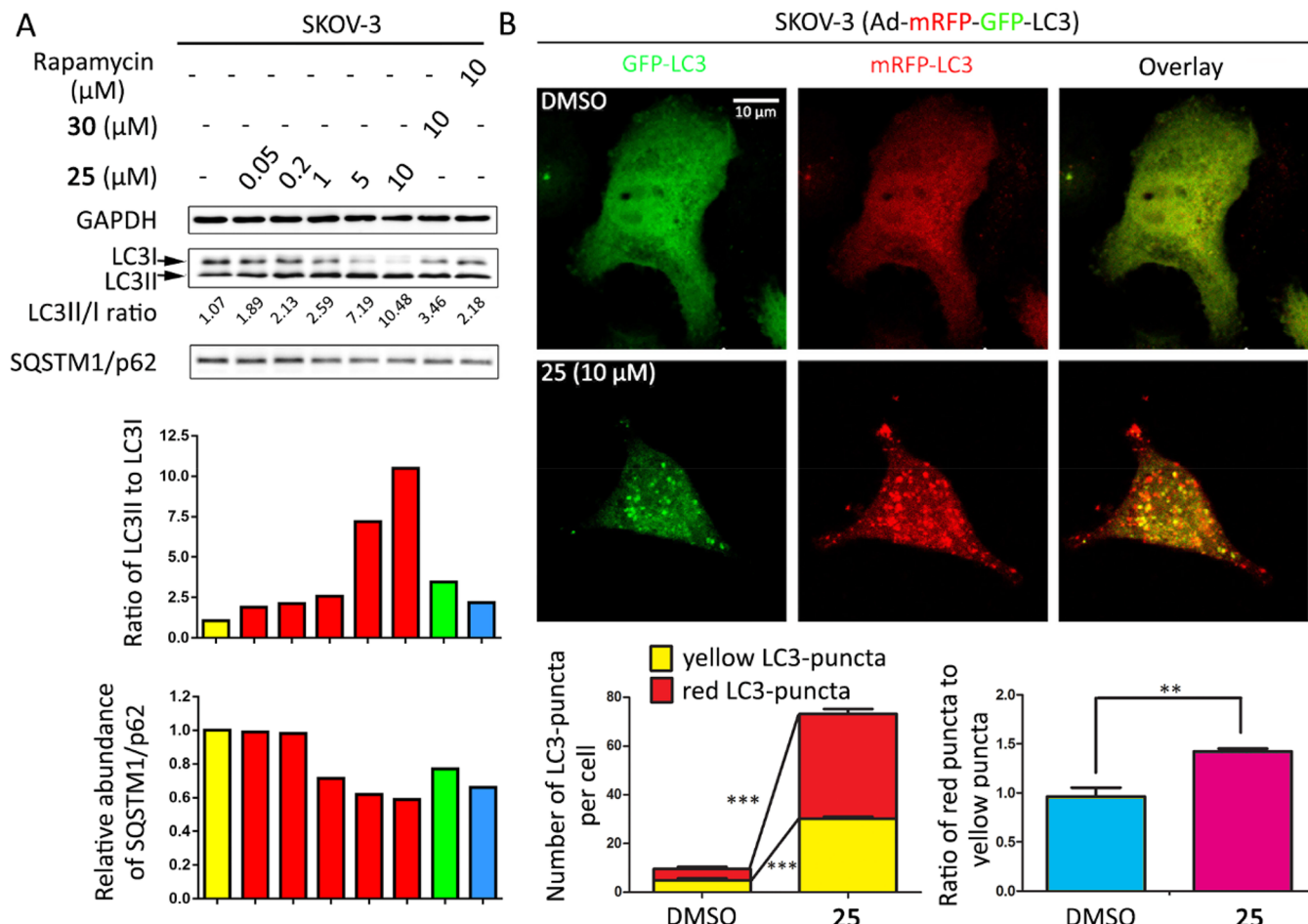


Figure 5. Detection of autophagy and autophagic flux induced by **25** in SKOV-3 cells. (A) SKOV-3 cells were treated with rapamycin (positive control), **30** (positive control), and various concentrations of **25** (0.05, 0.2, 1, 5, and 10 μ M) for 24 h. Then whole cell lysates were subjected to an immunoblotting assay to detect LC3 and SQSTM1/p62. Immunoblots were quantified as shown below. (B) Ad-mRFP-GFP-LC3-infected SKOV-3 cells were treated with **25** (10 μ M) for 24 h and fixed before examination by confocal microscopy. Representative photographs are presented. Scale bar: 10 μ m. Alignment of green and red signals appears yellow. The number of LC3-puncta (mean \pm SEM) in overlays was quantified and is shown below. More than 80 cells were counted in each individual experiment ($n = 3$). *** $P < 0.001$, ** $P < 0.01$.

Hz, 1H), 3.02 (d, $J = 5.0$ Hz, 3H). ^{13}C NMR (101 MHz, DMSO- d_6) δ 147.89, 147.33, 147.29, 135.10, 131.84, 126.97, 126.88, 121.73, 119.33, 34.20. ESI-MS m/z 281.9 [$\text{M} + \text{H}]^+$.

4.1.6. 6-Bromo-N-methyl-3-nitroquinolin-4-amine (6b). The title compound was prepared from **5** (1 g, 3.48 mmol) and commercial available ethanamine hydrochloride (284 mg, 3.48 mmol) using the procedure described for compound **6a** in 95% yield as an off-white powder. ^1H NMR (400 MHz, DMSO- d_6) δ 8.97 (d, $J = 2.6$ Hz, 1H), 8.74 (s, 1H), 8.61 (s, 1H), 7.97–7.89 (m, 1H), 7.84–7.76 (m, 1H), 3.44–3.35 (m, 2H), 1.29 (t, $J = 7.1$ Hz, 3H). ESI-MS m/z 296.0 [$\text{M} + \text{H}]^+$.

4.1.7. 6-Bromo-N-isopropyl-3-nitroquinolin-4-amine (6c). The title compound was prepared from **5** (1 g, 3.48 mmol) and commercial available propan-2-amine (298 μ L, 3.48 mmol) using the procedure described for compound **6a** in 93% yield as an off-white powder. ^1H NMR (400 MHz, DMSO- d_6) δ 8.99 (s, 1H), 8.71 (s, 1H), 8.31 (d, $J = 7.5$ Hz, 1H), 7.96 (d, $J = 8.3$ Hz, 1H), 7.83 (d, $J = 8.8$ Hz, 1H), 4.03–3.80 (m, 1H), 1.32 (d, $J = 6.0$ Hz, 6H). ESI-MS m/z 310.0 [$\text{M} + \text{H}]^+$.

4.1.8. 6-Bromo-N-(4-fluorobenzyl)-3-nitroquinolin-4-amine (6d). The title compound was prepared from **5** (750 mg, 2.61 mmol) and commercial available (4-fluorophenyl)methanamine (327 mg, 2.61 mmol) using the procedure described for compound **6a** in 91% yield as an off-white powder. ^1H NMR (400 MHz, DMSO- d_6) δ 9.20 (t, $J = 5.4$ Hz, 1H), 8.94 (s, 1H), 8.75 (d, $J = 1.9$ Hz, 1H), 7.96 (dd, $J = 8.9, 1.9$ Hz, 1H), 7.83 (d, $J = 8.9$ Hz, 1H), 7.35 (dd, $J = 8.7, 5.5$ Hz, 2H),

7.23–7.10 (m, 2H), 4.70 (d, $J = 5.7$ Hz, 2H). ESI-MS m/z 376.0 [$\text{M} + \text{H}]^+$.

4.1.9. (S)-6-Bromo-N-(1-(4-fluorophenyl)ethyl)-3-nitroquinolin-4-amine (6e). The title compound was prepared from **5** (5 g, 17.39 mmol) and commercial available (S)-1-(4-fluorophenyl)ethan-1-amine (2.42 g, 17.39 mmol) using the procedure described for compound **6a** in 93% yield as an off-white powder. ^1H NMR (400 MHz, DMSO- d_6) δ 8.96 (s, 1H), 8.86 (d, $J = 6.5$ Hz, 1H), 8.70 (d, $J = 1.9$ Hz, 1H), 7.94 (dd, $J = 8.8, 2.0$ Hz, 1H), 7.81 (d, $J = 8.8$ Hz, 1H), 7.42–7.36 (m, 2H), 7.19–7.11 (m, 2H), 5.10 (quint, $J = 6.6$ Hz, 1H), 1.66 (d, $J = 6.6$ Hz, 3H). ^{13}C NMR (101 MHz, DMSO- d_6) δ 163.02, 160.60, 148.01, 147.58, 146.42, 139.45, 139.42, 135.60, 131.93, 128.55, 128.46, 128.34, 128.13, 121.57, 119.58, 116.12, 115.91, 56.60, 25.85. ESI-MS m/z 390.0 [$\text{M} + \text{H}]^+$.

4.1.10. (R)-6-Bromo-N-(1-(4-fluorophenyl)ethyl)-3-nitroquinolin-4-amine (6f). The title compound was prepared from **5** (1 g, 3.48 mmol) and commercial available (R)-1-(4-fluorophenyl)ethan-1-amine (484 mg, 3.48 mmol) using the procedure described for compound **6a** in 92% yield as an off-white powder. ^1H NMR (400 MHz, DMSO- d_6) δ 8.96 (s, 1H), 8.86 (d, $J = 6.7$ Hz, 1H), 8.70 (d, $J = 1.9$ Hz, 1H), 7.94 (dd, $J = 8.9, 2.1$ Hz, 1H), 7.81 (d, $J = 8.8$ Hz, 1H), 7.43–7.33 (m, 2H), 7.20–7.10 (m, 2H), 5.15–5.06 (m, 1H), 1.66 (d, $J = 6.6$ Hz, 3H). ESI-MS m/z 390.0 [$\text{M} + \text{H}]^+$.

4.1.11. (S)-6-Bromo-3-nitro-N-(1-phenylethyl)quinolin-4-amine (6g). The title compound was prepared from **5** (1 g, 3.48 mmol) and commercial available (S)-1-phenylethan-1-amine (422 mg, 3.48

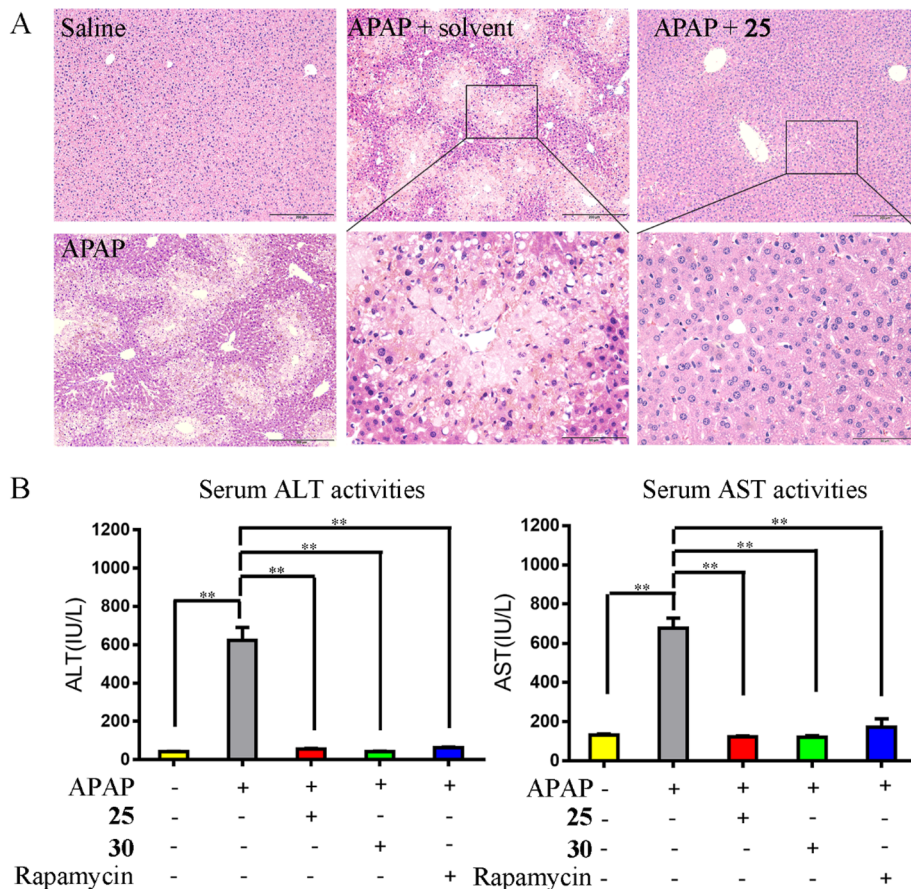


Figure 6. Protective effect of **25** on APAP-induced liver injury in mice. Male C57BL/6 mice were injected (ip) with **25** (30 mg/kg), **30** (30 mg/kg, positive control), rapamycin (30 mg/kg, positive control), or solvent (12.5% ethanol and 12.5% castor oil, 10 mL/kg), immediately followed by APAP (500 mg/kg) injection (ip) for 6 h. (A) Representative photographs of H&E staining are presented. (B) Serum ALT and AST levels were quantified ($n = 3$ mice). *** $P < 0.01$.

mmol) using the procedure described for compound **6a** in 90% yield as an off-white powder. ^1H NMR (400 MHz, DMSO- d_6) δ 8.98 (s, 1H), 8.70 (d, $J = 1.7$ Hz, 1H), 7.93 (dd, $J = 8.9, 2.0$ Hz, 1H), 7.80 (d, $J = 8.8$ Hz, 1H), 7.40–7.29 (m, 2H), 7.28–7.20 (m, 1H), 5.13 (quint, $J = 6.7$ Hz, 1H), 1.67 (d, $J = 6.6$ Hz, 2H). ESI-MS m/z 372.0 [M + H] $^+$.

4.1.12. (R)-6-Bromo-3-nitro-N-(1-phenylethyl)quinolin-4-amine (6h). The title compound was prepared from **5** (1 g, 3.48 mmol) and commercial available (R)-1-phenylethan-1-amine (422 mg, 3.48 mmol) using the procedure described for compound **6a** in 91% yield as an off-white powder. ^1H NMR (400 MHz, DMSO- d_6) δ 8.98 (s, 2H), 8.69 (s, 1H), 7.93 (dd, $J = 8.8, 1.9$ Hz, 1H), 7.80 (d, $J = 8.8$ Hz, 1H), 7.33 (q, $J = 8.2$ Hz, 4H), 7.25 (t, $J = 6.8$ Hz, 1H), 5.23–5.07 (m, 1H), 1.67 (d, $J = 6.6$ Hz, 3H). ESI-MS m/z 372.0 [M + H] $^+$.

4.1.13. (S)-6-Bromo-3-nitro-N-(1-(*p*-tolyl)ethyl)quinolin-4-amine (6i). The title compound was prepared from **5** (1 g, 3.48 mmol) and commercial available (S)-1-(*p*-tolyl)ethan-1-amine (470 mg, 3.48 mmol) using the procedure described for compound **6a** in 90% yield as an off-white powder. ^1H NMR (400 MHz, DMSO- d_6) δ 8.97 (s, 2H), 8.71 (s, 1H), 7.92 (d, $J = 8.8$ Hz, 1H), 7.80 (d, $J = 8.1$ Hz, 1H), 7.22 (d, $J = 8.1$ Hz, 2H), 7.12 (d, $J = 8.0$ Hz, 2H), 5.16–5.03 (m, 1H), 2.25 (s, 3H), 1.64 (d, $J = 6.6$ Hz, 3H). ESI-MS m/z 386.0 [M + H] $^+$.

4.1.14. (R)-6-Bromo-3-nitro-N-(1-(*p*-tolyl)ethyl)quinolin-4-amine (6j). The title compound was prepared from **5** (1 g, 3.48 mmol) and commercial available (R)-1-(*p*-tolyl)ethan-1-amine (470 mg, 3.48 mmol) using the procedure described for compound **6a** in 92% yield as an off-white powder. ^1H NMR (400 MHz, DMSO- d_6) δ 8.96 (d, $J = 9.0$ Hz, 2H), 8.71 (s, 1H), 7.93 (dd, $J = 8.9, 1.9$ Hz, 1H), 7.80 (d, $J = 8.8$ Hz, 1H), 7.22 (d, $J = 8.0$ Hz, 2H), 7.12 (d, $J = 8.0$ Hz, 2H), 5.09 (quint, $J = 6.5$ Hz, 1H), 2.25 (s, 3H), 1.64 (d, $J = 6.6$ Hz, 3H). ESI-MS m/z 386.0 [M + H] $^+$.

4.1.15. (S)-6-Bromo-N-(1-(4-chlorophenyl)ethyl)-3-nitroquinolin-4-amine (6k). The title compound was prepared from **5** (900 mg, 3.13 mmol) and commercial available (S)-1-(4-chlorophenyl)ethan-1-amine (487 mg, 3.13 mmol) using the procedure described for compound **6a** in 93% yield as an off-white powder. ^1H NMR (400 MHz, DMSO- d_6) δ 8.96 (s, 1H), 8.83 (d, $J = 6.2$ Hz, 1H), 8.71 (s, 1H), 7.94 (d, $J = 8.9$ Hz, 1H), 7.82 (d, $J = 8.8$ Hz, 1H), 7.38 (s, 4H), 5.13–5.00 (m, 1H), 1.65 (d, $J = 6.6$ Hz, 3H). ESI-MS m/z 405.9 [M + H] $^+$.

4.1.16. 8-Bromo-1-methyl-1H-[1,2,3]triazolo[4,5-*c*]quinolone (8a). To a stirred solution of **6a** (1 g, 3.54 mmol, 1 equiv) in AcOH (30 mL), Fe powder (989.82 mg, 17.72 mmol, 5 equiv) was added in several batches at 60 °C. Upon completion of the reaction, the mixture was cooled to rt. The crude product **7a** was used for the next step without further purification.

The reaction flask was transferred into an ice–water bath, and 60 mL of water was poured into the mixture. Concentrated hydrochloric acid was used to adjust the pH to 2–3. Then, a 0.5 mol/L aqueous solution of sodium nitrite (10.64 mL, 5.32 mmol, 1.5 equiv) was added dropwise into the solution under vigorous stirring. The resulting solution was stirred for another 30 min at rt. Then, a large amount of water was added, and the pH was adjusted to 5–6. The aqueous phase was extracted with ethyl acetate. The combined organic phase was separated, dried over anhydrous sodium sulfate, and filtered. The filtrate was evaporated to dryness under reduced pressure to yield a solid residue, which was purified by flash column chromatography to yield the desired product as a white powder (730.3 mg, two-step yield 78%). ^1H NMR (400 MHz, CDCl₃) δ 9.54 (s, 1H), 8.47 (d, $J = 2.1$ Hz, 1H), 8.21 (d, $J = 8.9$ Hz, 1H), 7.93 (dd, $J = 8.9, 2.1$ Hz, 1H), 4.71 (s, 3H). ^{13}C NMR (101 MHz, CDCl₃) δ 145.45, 144.20, 141.28,

133.04, 132.62, 123.94, 121.75, 117.02, 100.00, 37.60. ESI-MS *m/z* 262.9 [M + H]⁺.

4.1.17. *S*-Bromo-1-ethyl-1*H*-[1,2,3]triazolo[4,5-*c*]quinolone (8b**).** The title compound was prepared from **6b** (600 mg, 2.03 mmol) in 76% yield as a pale-yellow powder according to the procedure described for compound **8a**. ¹H NMR (400 MHz, DMSO-*d*₆) δ 9.58 (s, 1H), 8.63 (d, *J* = 2.1 Hz, 1H), 8.19 (d, *J* = 8.9 Hz, 1H), 8.05 (dd, *J* = 8.9, 2.2 Hz, 1H), 5.16 (q, *J* = 7.3 Hz, 2H), 1.63 (t, *J* = 7.3 Hz, 3H). ¹³C NMR (101 MHz, DMSO-*d*₆) δ 145.78, 144.07, 141.18, 133.23, 132.68, 131.92, 125.34, 121.54, 117.07, 45.92, 15.06. ESI-MS *m/z* 277.0 [M + H]⁺.

4.1.18. *S*-Bromo-1-isopropyl-1*H*-[1,2,3]triazolo[4,5-*c*]quinolone (8c**).** The title compound was prepared from **6c** (600 mg, 1.93 mmol) in 75% yield as a white powder according to the procedure described for compound **8a**. ¹H NMR (400 MHz, DMSO-*d*₆) δ 9.60 (s, 1H), 8.70 (s, 1H), 8.21 (d, *J* = 8.9 Hz, 1H), 8.06 (dd, *J* = 8.8, 1.3 Hz, 1H), 5.80–5.67 (m, 1H), 1.75 (d, *J* = 6.5 Hz, 6H). ¹³C NMR (101 MHz, DMSO-*d*₆) δ 145.81, 144.14, 140.87, 133.08, 132.78, 131.58, 125.15, 121.58, 117.15, 53.66, 22.77. ESI-MS *m/z* 291.0 [M + H]⁺.

4.1.19. *S*-Bromo-1-(4-fluorobenzyl)-1*H*-[1,2,3]triazolo[4,5-*c*]quinolone (8d**).** The title compound was prepared from **6d** (500 mg, 1.33 mmol) in 73% yield as an off-white powder according to the procedure described for compound **8a**. ¹H NMR (400 MHz, CDCl₃) δ 9.58 (s, 1H), 8.28–8.13 (m, 2H), 7.86 (dd, *J* = 8.9, 2.1 Hz, 1H), 7.22 (dd, *J* = 8.5, 5.1 Hz, 2H), 7.07 (t, *J* = 8.5 Hz, 2H), 6.21 (s, 2H). ¹³C NMR (101 MHz, DMSO-*d*₆) δ 163.47, 161.03, 145.85, 144.19, 141.42, 133.34, 132.57, 132.33, 131.77, 131.74, 129.54, 129.45, 125.79, 121.31, 116.60, 116.51, 116.30, 52.69. ESI-MS *m/z* 357.0 [M + H]⁺.

4.1.20. (*S*)-(–)-*S*-Bromo-1-(1-(4-fluorophenyl)ethyl)-1*H*-[1,2,3]triazolo[4,5-*c*]quinolone (8e**).** The title compound was prepared from **6e** (1 g, 2.56 mmol) in 75% yield as a white powder according to the procedure described for compound **8a**; $[\alpha]_D^{25} = -220.78$ (*c* = 0.361, CH₃Cl). ¹H NMR (400 MHz, DMSO-*d*₆) δ 9.65 (s, 1H), 8.54 (d, *J* = 2.0 Hz, 1H), 8.16 (d, *J* = 8.9 Hz, 1H), 7.99 (dd, *J* = 8.9, 1.9 Hz, 1H), 7.35–7.24 (m, 2H), 7.19 (t, *J* = 8.8 Hz, 2H), 6.93 (q, *J* = 6.7 Hz, 1H), 2.18 (d, *J* = 6.8 Hz, 3H). ¹³C NMR (101 MHz, DMSO-*d*₆) δ 163.28, 160.85, 145.93, 144.22, 141.24, 137.50, 133.21, 132.68, 132.19, 128.58, 128.49, 125.75, 121.36, 116.73, 116.51, 116.30, 59.85, 23.33. ESI-MS *m/z* 371.0 [M + H]⁺.

4.1.21. (*R*)-(+)-*S*-Bromo-1-(1-(4-fluorophenyl)ethyl)-1*H*-[1,2,3]triazolo[4,5-*c*]quinolone (8f**).** The title compound was prepared from **6f** (600 mg, 1.54 mmol) in 73% yield as an off-white powder according to the procedure described for compound **8a**; $[\alpha]_D^{25} = 218.22$ (*c* = 0.105, CH₃Cl). ¹H NMR (400 MHz, DMSO-*d*₆) δ 9.65 (s, 1H), 8.54 (d, *J* = 2.0 Hz, 1H), 8.16 (d, *J* = 8.9 Hz, 1H), 7.99 (dd, *J* = 8.9, 1.8 Hz, 1H), 7.33–7.25 (m, 2H), 7.19 (t, *J* = 8.8 Hz, 2H), 6.93 (q, *J* = 6.8 Hz, 1H), 2.17 (d, *J* = 6.8 Hz, 3H). ¹³C NMR (101 MHz, DMSO-*d*₆) δ 163.28, 160.85, 145.90, 144.20, 141.22, 137.49, 137.46, 133.17, 132.65, 132.17, 128.57, 128.49, 125.73, 121.35, 116.71, 116.50, 116.29, 59.86, 23.33. ESI-MS *m/z* 371.0 [M + H]⁺.

4.1.22. (*S*)-*S*-Bromo-1-(1-phenylethyl)-1*H*-[1,2,3]triazolo[4,5-*c*]quinolone (8g**).** The title compound was prepared from **6g** (600 mg, 1.61 mmol) in 69% yield as an off-white powder according to the procedure described for compound **8a**. ¹H NMR (400 MHz, DMSO-*d*₆) δ 9.65 (s, 1H), 8.50 (d, *J* = 1.8 Hz, 1H), 8.15 (d, *J* = 8.8 Hz, 1H), 7.97 (d, *J* = 8.9 Hz, 1H), 7.35 (t, *J* = 7.4 Hz, 2H), 7.27 (t, *J* = 7.3 Hz, 1H), 7.24–7.16 (m, 2H), 6.89 (q, *J* = 6.7 Hz, 1H), 2.19 (d, *J* = 6.8 Hz, 3H). ¹³C NMR (101 MHz, DMSO-*d*₆) δ 145.91, 144.17, 141.35, 141.25, 133.11, 132.61, 132.25, 129.58, 128.51, 126.17, 125.87, 121.26, 116.73, 60.58, 23.36. ESI-MS *m/z* 353.0 [M + H]⁺.

4.1.23. (*R*)-*S*-Bromo-1-(1-phenylethyl)-1*H*-[1,2,3]triazolo[4,5-*c*]quinolone (8h**).** The title compound was prepared from **6h** (600 mg, 1.61 mmol) in 79% yield as a pale-yellow powder according to the procedure described for compound **8a**. ¹H NMR (400 MHz, DMSO-*d*₆) δ 9.65 (s, 1H), 8.51 (d, *J* = 2.1 Hz, 1H), 8.14 (d, *J* = 8.9 Hz, 1H), 7.96 (dd, *J* = 8.9, 2.1 Hz, 1H), 7.36 (dd, *J* = 10.1, 4.6 Hz, 2H), 7.32–7.25 (m, 1H), 7.25–7.16 (m, 2H), 6.89 (q, *J* = 6.7 Hz, 1H), 2.20 (d, *J* = 6.8 Hz, 3H). ¹³C NMR (101 MHz, DMSO-*d*₆) δ 145.91, 144.18, 141.34, 141.25, 133.11, 132.60, 132.25, 129.58, 128.51, 126.17, 125.87, 121.25, 116.73, 60.59, 23.35. ESI-MS *m/z* 353.0 [M + H]⁺.

4.1.24. (*S*)-*S*-Bromo-1-(1-(*p*-tolyl)ethyl)-1*H*-[1,2,3]triazolo[4,5-*c*]quinolone (8i**).** The title compound was prepared from **6i** (500 mg, 1.29 mmol) in 77% yield as an off-white powder according to the procedure described for compound **8a**. ¹H NMR (400 MHz, CDCl₃) δ 9.57 (s, 1H), 8.28 (d, *J* = 2.1 Hz, 1H), 8.13 (d, *J* = 8.9 Hz, 1H), 7.81 (dd, *J* = 8.9, 2.1 Hz, 1H), 7.16 (d, *J* = 8.1 Hz, 2H), 7.11 (d, *J* = 8.2 Hz, 2H), 6.34 (q, *J* = 6.8 Hz, 1H), 2.29 (d, *J* = 6.8 Hz, 6H), 2.30 (s, 3H). ¹³C NMR (101 MHz, DMSO-*d*₆) δ 145.92, 144.17, 141.24, 138.41, 137.82, 133.11, 132.61, 132.20, 130.09, 126.08, 125.93, 121.26, 116.75, 60.42, 23.41, 21.03. ESI-MS *m/z* 367.0 [M + H]⁺.

4.1.25. (*R*)-*S*-Bromo-1-(1-(*p*-tolyl)ethyl)-1*H*-[1,2,3]triazolo[4,5-*c*]quinolone (8j**).** The title compound was prepared from **6j** (600 mg, 1.55 mmol) in 74% yield as an off-white powder according to the procedure described for compound **8a**. ¹H NMR (400 MHz, DMSO-*d*₆) δ 9.64 (s, 1H), 8.52 (d, *J* = 2.1 Hz, 1H), 8.15 (d, *J* = 8.9 Hz, 1H), 7.97 (dd, *J* = 8.9, 2.1 Hz, 1H), 7.14 (d, *J* = 8.1 Hz, 2H), 7.09 (d, *J* = 8.2 Hz, 2H), 6.84 (q, *J* = 6.7 Hz, 1H), 2.22 (s, 3H), 2.16 (d, *J* = 6.8 Hz, 3H). ¹³C NMR (101 MHz, DMSO-*d*₆) δ 145.92, 144.17, 141.24, 138.41, 137.82, 133.11, 132.61, 132.20, 130.10, 126.08, 125.93, 121.26, 116.76, 60.42, 23.41, 21.03. ESI-MS *m/z* 367.0 [M + H]⁺.

4.1.26. (*S*)-(–)-*S*-Bromo-1-(1-(4-chlorophenyl)ethyl)-1*H*-[1,2,3]triazolo[4,5-*c*]quinolone (8k**).** The title compound was prepared from **6k** (500 mg, 1.23 mmol) in 77% yield as an off-white powder according to the procedure described for compound **8a**. ¹H NMR (400 MHz, CDCl₃) δ 9.58 (s, 1H), 8.23 (d, *J* = 1.8 Hz, 1H), 8.17 (dd, *J* = 8.8, 3.7 Hz, 1H), 7.89–7.79 (m, 1H), 7.39–7.31 (m, 2H), 7.17 (d, *J* = 8.5 Hz, 2H), 6.36 (q, *J* = 6.9 Hz, 1H), 2.32 (d, *J* = 7.0 Hz, 3H). ¹³C NMR (101 MHz, DMSO-*d*₆) δ 145.90, 144.21, 141.22, 140.25, 133.20, 133.17, 132.66, 132.21, 129.55, 128.28, 125.67, 121.38, 116.69, 59.84, 23.15. ESI-MS *m/z* 386.9 [M + H]⁺.

4.1.27. 1-Ethyl-8-(2-methylpyridin-4-yl)-1*H*-[1,2,3]triazolo[4,5-*c*]quinoline (9b**).** The title compound was prepared from **8b** (50 mg, 180 μ mol) and **29** (25 mg, 180 μ mol) using the procedure described for compound **1** in 76% yield as an off-white powder. ¹H NMR (400 MHz, DMSO-*d*₆) δ 9.58 (s, 1H), 8.68 (d, *J* = 1.5 Hz, 1H), 8.61 (d, *J* = 5.2 Hz, 1H), 8.36 (d, *J* = 8.7 Hz, 1H), 8.26 (dd, *J* = 8.7, 1.7 Hz, 1H), 7.80 (s, 1H), 7.75 (d, *J* = 5.1 Hz, 1H), 5.27 (q, *J* = 7.2 Hz, 2H), 2.61 (s, 3H), 1.69 (t, *J* = 7.2 Hz, 3H). ¹³C NMR (101 MHz, DMSO-*d*₆) δ 159.28, 150.18, 146.78, 145.85, 145.41, 141.25, 137.29, 132.83, 131.43, 128.75, 121.66, 121.22, 119.62, 115.95, 46.03, 24.70, 15.02. ESI-MS *m/z* 290.1 [M + H]⁺.

4.1.28. 1-Isopropyl-8-(2-methylpyridin-4-yl)-1*H*-[1,2,3]triazolo[4,5-*c*]quinoline (9c**).** The title compound was prepared from **8c** (50 mg, 172 μ mol) and **29** (24 mg, 172 μ mol) using the procedure described for compound **1** in 80% yield as an off-white powder. ¹H NMR (400 MHz, CDCl₃) δ 9.59 (s, 1H), 8.67 (d, *J* = 5.2 Hz, 1H), 8.49 (d, *J* = 1.9 Hz, 1H), 8.45 (d, *J* = 8.7 Hz, 1H), 8.06 (dd, *J* = 8.7, 2.0 Hz, 1H), 7.49 (s, 1H), 7.44 (dd, *J* = 5.2, 1.4 Hz, 1H), 5.53 (m, 1H), 2.71 (s, 3H), 1.96 (d, *J* = 6.6 Hz, 6H). ¹³C NMR (101 MHz, DMSO-*d*₆) δ 159.27, 150.19, 146.87, 145.99, 145.54, 141.02, 137.38, 132.58, 131.62, 128.73, 121.73, 121.16, 119.70, 116.12, 53.77, 24.74, 22.77. ESI-MS *m/z* 304.2 [M + H]⁺.

4.1.29. 1-(4-Fluorobenzyl)-8-(2-methylpyridin-4-yl)-1*H*-[1,2,3]triazolo[4,5-*c*]quinolone (9d**).** The title compound was prepared from **8d** (50 mg, 140 μ mol) and **29** (19 mg, 140 μ mol) using the procedure described for compound **1** in 84% yield as a pale-yellow powder. ¹H NMR (400 MHz, DMSO-*d*₆) δ 9.67 (s, 1H), 8.60 (d, *J* = 5.2 Hz, 1H), 8.45 (s, 1H), 8.34 (d, *J* = 8.7 Hz, 1H), 8.24 (d, *J* = 8.6 Hz, 1H), 7.54 (d, *J* = 4.9 Hz, 1H), 7.49 (s, 1H), 7.38–7.29 (m, 2H), 7.23 (t, *J* = 8.8 Hz, 2H), 6.57 (s, 2H), 2.60 (s, 3H). ¹³C NMR (101 MHz, DMSO-*d*₆) δ 162.95, 160.52, 158.76, 149.70, 145.94, 145.48, 145.06, 141.07, 136.42, 132.77, 131.57, 130.82, 128.82, 128.74, 128.29, 121.36, 120.87, 118.81, 116.10, 115.89, 115.02, 52.29, 24.18. ESI-MS *m/z* 370.1 [M + H]⁺.

4.1.30. (*S*)-(–)-1-(1-(4-Fluorophenyl)ethyl)-8-(2-methylpyridin-4-yl)-1*H*-[1,2,3]triazolo[4,5-*c*]quinolone (9e**).** The title compound was prepared from **8e** (50 mg, 135 μ mol) and **29** (19 mg, 135 μ mol) using the procedure described for compound **1** in 85% yield as a white powder; $[\alpha]_D^{25} = -188.72$ (*c* = 0.133, CH₃Cl). ¹H NMR (400 MHz, DMSO-*d*₆) δ 9.67 (s, 1H), 8.63 (d, *J* = 5.1 Hz, 1H), 8.52 (d, *J* = 1.8

Hz, 1H), 8.33 (d, J = 8.7 Hz, 1H), 8.22 (dd, J = 8.7, 2.0 Hz, 1H), 7.60–7.57 (m, 1H), 7.56 (s, 1H), 7.38–7.30 (m, 2H), 7.26–7.17 (m, 2H), 7.05 (q, J = 6.7 Hz, 1H), 2.64 (s, 3H), 2.23 (d, J = 6.8 Hz, 3H). ^{13}C NMR (101 MHz, DMSO- d_6) δ 163.26, 160.83, 159.28, 150.20, 146.46, 146.04, 145.59, 141.40, 137.97, 137.94, 136.89, 133.18, 131.43, 128.62, 128.41, 128.32, 121.74, 121.38, 119.34, 116.63, 116.41, 115.65, 60.13, 24.70, 23.59. ESI-MS m/z : 384.1 [M + H]⁺. HPLC analysis ($\text{H}_2\text{O}/\text{MeCN} = 4/6$, $t_{\text{R}} = 18.09$ min).

4.1.31. (*R*)-(+)-1-(1-(4-Fluorophenyl)ethyl)-8-(2-methylpyridin-4-yl)-1*H*-[1,2,3]triazolo[4,5-*c*]quinolone (**9f**). The title compound was prepared from **8f** (50 mg, 135 μmol) and **29** (19 mg, 135 μmol) using the procedure described for compound **1** in 87% yield as an off-white powder; $[\alpha]_{\text{D}}^{25} = 187.85$ ($c = 0.109$, CH_3Cl). ^1H NMR (400 MHz, DMSO- d_6) δ 9.67 (s, 1H), 8.62 (d, J = 5.2 Hz, 1H), 8.51 (d, J = 1.6 Hz, 1H), 8.34 (d, J = 8.7 Hz, 1H), 8.23 (d, J = 8.7 Hz, 1H), 7.58 (d, J = 5.2 Hz, 1H), 7.56 (s, 1H), 7.37–7.28 (m, 2H), 7.21 (t, J = 8.8 Hz, 2H), 7.04 (q, J = 6.7 Hz, 1H), 2.63 (s, 3H), 2.22 (d, J = 6.8 Hz, 3H). ^{13}C NMR (101 MHz, DMSO- d_6) δ 162.75, 160.32, 158.79, 149.71, 145.96, 145.56, 145.10, 140.91, 137.46, 137.43, 136.41, 132.69, 130.95, 128.14, 127.90, 127.82, 121.25, 120.88, 118.85, 116.12, 115.91, 115.16, 59.62, 24.20, 23.88, 23.09. ESI-MS m/z : 384.4 [M + H]⁺.

4.1.32. (*S*)-(−)-8-(2-Methylpyridin-4-yl)-1-(1-phenylethyl)-1*H*-[1,2,3]triazolo[4,5-*c*]quinolone (**9g**). The title compound was prepared from **8g** (55 mg, 156 μmol) and **29** (21 mg, 156 μmol) using the procedure described for compound **1** in 91% yield as an off-white powder; $[\alpha]_{\text{D}}^{25} = -178.67$ ($c = 0.147$, CH_3Cl). ^1H NMR (400 MHz, DMSO- d_6) δ 9.67 (s, 1H), 8.60 (d, J = 5.2 Hz, 1H), 8.49 (d, J = 1.7 Hz, 1H), 8.32 (d, J = 8.6 Hz, 1H), 8.21 (d, J = 8.7 Hz, 1H), 7.53 (d, J = 5.3 Hz, 1H), 7.52 (s, 1H), 7.37 (t, J = 7.5 Hz, 2H), 7.29 (d, J = 7.3 Hz, 1H), 7.27–7.22 (m, 2H), 7.01 (q, J = 6.6 Hz, 1H), 2.62 (s, 3H), 2.23 (d, J = 6.8 Hz, 3H). ^{13}C NMR (101 MHz, DMSO- d_6) δ 159.25, 150.17, 146.48, 146.07, 145.57, 141.83, 141.43, 136.78, 133.26, 131.38, 129.70, 128.55, 128.51, 126.06, 121.97, 121.34, 119.33, 115.68, 60.82, 24.69, 23.60. ESI-MS m/z : 366.2 [M + H]⁺.

4.1.33. (*R*)-(+)-8-(2-Methylpyridin-4-yl)-1-(1-phenylethyl)-1*H*-[1,2,3]triazolo[4,5-*c*]quinolone (**9h**). The title compound was prepared from **8h** (50 mg, 142 μmol) and **29** (19 mg, 142 μmol) using the procedure described for compound **1** in 92% yield as a white powder; $[\alpha]_{\text{D}}^{25} = 180.43$ ($c = 0.111$, CH_3Cl). ^1H NMR (400 MHz, DMSO- d_6) δ 9.67 (s, 1H), 8.60 (d, J = 5.1 Hz, 1H), 8.49 (s, 1H), 8.32 (d, J = 8.7 Hz, 1H), 8.20 (dd, J = 8.7, 1.6 Hz, 1H), 7.53 (d, J = 5.6 Hz, 1H), 7.52 (s, 1H), 7.37 (t, J = 7.5 Hz, 2H), 7.29 (d, J = 7.2 Hz, 1H), 7.25 (d, J = 7.5 Hz, 2H), 7.01 (q, J = 6.7 Hz, 1H), 2.62 (s, 3H), 2.23 (d, J = 6.8 Hz, 3H). ^{13}C NMR (101 MHz, DMSO- d_6) δ 159.25, 150.17, 146.48, 146.07, 145.57, 141.83, 141.43, 136.78, 133.26, 131.38, 129.70, 128.55, 128.51, 126.06, 121.97, 121.34, 119.33, 115.68, 60.82, 24.69, 23.60. ESI-MS m/z : 366.2 [M + H]⁺.

4.1.34. (*S*)-(−)-8-(2-Methylpyridin-4-yl)-1-(1-(*p*-tolyl)ethyl)-1*H*-[1,2,3]triazolo[4,5-*c*]quinolone (**9i**). The title compound was prepared from **8i** (52 mg, 142 μmol) and **29** (20 mg, 142 μmol) using the procedure described for compound **1** in 91% yield as an off-white powder; $[\alpha]_{\text{D}}^{25} = -228.32$ ($c = 0.113$, CH_3Cl). ^1H NMR (400 MHz, DMSO- d_6) δ 9.66 (s, 1H), 8.61 (d, J = 5.2 Hz, 1H), 8.51 (d, J = 1.8 Hz, 1H), 8.32 (d, J = 8.7 Hz, 1H), 8.21 (dd, J = 8.7, 2.0 Hz, 1H), 7.56 (d, J = 5.2 Hz, 1H), 7.53 (s, 1H), 7.15 (q, J = 8.2 Hz, 4H), 6.96 (q, J = 6.7 Hz, 1H), 2.63 (s, 3H), 2.21 (s, 3H), 2.20 (d, J = 6.8 Hz, 3H). ^{13}C NMR (101 MHz, DMSO- d_6) δ 158.76, 149.69, 146.01, 145.56, 145.07, 140.91, 138.36, 137.32, 136.28, 132.71, 130.87, 129.70, 128.05, 125.47, 121.52, 120.87, 118.85, 115.20, 60.15, 24.18, 23.13, 20.51. ESI-MS m/z : 380.2 [M + H]⁺.

4.1.35. (*R*)-(+)-8-(2-Methylpyridin-4-yl)-1-(1-(*p*-tolyl)ethyl)-1*H*-[1,2,3]triazolo[4,5-*c*]quinolone (**9j**). The title compound was prepared from **8j** (50 mg, 136 μmol) and **29** (19 mg, 136 μmol) using the procedure described for compound **1** in 90% yield as a yellow powder; $[\alpha]_{\text{D}}^{25} = 227.81$ ($c = 0.119$, CH_3Cl). ^1H NMR (400 MHz, DMSO- d_6) δ 9.67 (s, 1H), 8.61 (d, J = 5.2 Hz, 1H), 8.51 (d, J = 1.8 Hz, 1H), 8.33 (d, J = 8.7 Hz, 1H), 8.22 (dd, J = 8.7, 2.0 Hz, 1H), 7.56 (dd, J = 5.2, 1.6 Hz, 1H), 7.53 (s, 1H), 7.15 (m, 4H), 6.96 (q, J = 6.7 Hz, 1H), 2.63 (s, 3H), 2.21 (d, J = 7.7 Hz, 6H). ESI-MS m/z : 380.2 [M + H]⁺.

4.1.36. (*S*)-(−)-1-(1-(4-Chlorophenyl)ethyl)-8-(2-methylpyridin-4-yl)-1*H*-[1,2,3]triazolo[4,5-*c*]quinolone (**9k**). The title compound was prepared from **8k** (50 mg, 129 μmol) and **29** (18 mg, 129 μmol) according to the procedure described for compound **1** in 87% yield as a white powder; $[\alpha]_{\text{D}}^{25} = -277.65$ ($c = 0.089$, CH_3Cl). ^1H NMR (400 MHz, DMSO- d_6) δ 9.67 (s, 1H), 8.62 (d, J = 5.2 Hz, 1H), 8.48 (s, 1H), 8.34 (d, J = 8.7 Hz, 1H), 8.23 (d, J = 8.7 Hz, 1H), 7.57 (d, J = 5.2 Hz, 1H), 7.52 (s, 1H), 7.44 (d, J = 8.5 Hz, 2H), 7.29 (d, J = 8.5 Hz, 2H), 7.04 (q, J = 6.7 Hz, 1H), 2.63 (s, 3H), 2.22 (d, J = 6.8 Hz, 3H). ^{13}C NMR (101 MHz, DMSO- d_6) δ 158.79, 149.72, 145.96, 145.57, 145.11, 140.92, 140.23, 136.43, 132.72, 132.62, 130.97, 129.18, 128.19, 127.65, 121.20, 120.88, 118.86, 115.14, 59.61, 24.20, 22.87. ESI-MS m/z : 400.1 [M + H]⁺.

4.1.37. (*S*)-1-(1-(4-Fluorophenyl)ethyl)-8-phenyl-1*H*-[1,2,3]triazolo[4,5-*c*]quinolone (**10**). The title compound was prepared from **8e** (50 mg, 135 μmol) and commercially available phenylboronic acid (17 mg, 135 μmol) according to the procedure described for compound **1** in 94% yield as a white powder. ^1H NMR (400 MHz, DMSO- d_6) δ 9.62 (s, 1H), 8.45 (d, J = 1.8 Hz, 1H), 8.30 (d, J = 8.7 Hz, 1H), 8.15 (dd, J = 8.7, 2.0 Hz, 1H), 7.73 (d, J = 7.2 Hz, 2H), 7.58 (t, J = 8.0 Hz, 2H), 7.52–7.44 (m, 1H), 7.36–7.26 (m, 2H), 7.26–7.17 (m, 2H), 7.02 (q, J = 6.7 Hz, 1H), 2.20 (d, J = 6.8 Hz, 3H). ^{13}C NMR (101 MHz, DMSO- d_6) δ 163.27, 160.84, 145.28, 144.83, 141.36, 139.33, 138.01, 133.17, 131.22, 129.65, 128.95, 128.69, 128.46, 128.38, 127.78, 121.10, 116.58, 116.37, 115.70, 60.13, 23.56. ESI-MS m/z : 369.1 [M + H]⁺.

4.1.38. (*S*)-1-(1-(4-Fluorophenyl)ethyl)-8-(6-(4-methylpiperazin-1-yl)pyridin-3-yl)-1*H*-[1,2,3]triazolo[4,5-*c*]quinolone (**11**). The title compound was prepared from **8e** (50 mg, 135 μmol) and commercially available (6-(4-methylpiperazin-1-yl)pyridin-3-yl)boronic acid (41 mg, 135 μmol) using the procedure described for compound **1** in 72% yield as a pale-yellow powder. ^1H NMR (400 MHz, DMSO- d_6) δ 9.56 (s, 1H), 8.59 (d, J = 2.5 Hz, 1H), 8.41 (d, J = 1.7 Hz, 1H), 8.25 (d, J = 8.7 Hz, 1H), 8.12 (dd, J = 8.7, 1.8 Hz, 1H), 7.93 (dd, J = 8.9, 2.6 Hz, 1H), 7.30 (dd, J = 8.7, 5.4 Hz, 2H), 7.19 (t, J = 8.8 Hz, 2H), 7.05 (t, J = 6.8 Hz, 1H), 7.02 (t, J = 4.0 Hz, 1H), 3.61 (d, J = 4.7 Hz, 4H), 2.46 (s, 4H), 2.26 (s, 3H), 2.20 (d, J = 6.4 Hz, 3H). ESI-MS m/z : 468.2 [M + H]⁺.

4.1.39. (*S*)-1-(1-(4-Fluorophenyl)ethyl)-8-(pyridin-4-yl)-1*H*-[1,2,3]triazolo[4,5-*c*]quinolone (**12**). The title compound was prepared from **8e** (50 mg, 135 μmol) and commercially available pyridin-4-ylboronic acid (17 mg, 135 μmol) using the procedure described for compound **1** in 93% yield as a white powder. ^1H NMR (400 MHz, CDCl_3) δ 9.68 (s, 1H), 8.77 (d, J = 5.1 Hz, 2H), 8.59 (s, 1H), 8.35 (d, J = 8.6 Hz, 1H), 8.26 (d, J = 8.6 Hz, 1H), 7.80 (d, J = 5.1 Hz, 2H), 7.38–7.28 (m, 1H), 7.21 (t, J = 8.6 Hz, 2H), 7.07 (q, J = 6.4 Hz, 1H), 2.22 (d, J = 6.6 Hz, 3H). ^{13}C NMR (101 MHz, DMSO- d_6) δ 163.27, 160.84, 150.91, 146.22, 146.15, 145.65, 141.39, 137.90, 136.67, 132.87, 131.54, 128.64, 128.51, 128.43, 122.20, 121.81, 116.62, 116.40, 115.70, 60.08, 23.53. ESI-MS m/z : 370.1 [M + H]⁺.

4.1.40. (*S*)-1-(1-(4-Fluorophenyl)ethyl)-8-(2-methoxypyridin-4-yl)-1*H*-[1,2,3]triazolo[4,5-*c*]quinolone (**13**). The title compound was prepared from **8e** (50 mg, 135 μmol) and commercially available (2-methoxypyridin-4-yl)boronic acid (21 mg, 135 μmol) using the procedure described for compound **1** in 90% yield as an off-white powder. ^1H NMR (400 MHz, DMSO- d_6) δ 9.67 (s, 1H), 8.54 (s, 1H), 8.43–8.26 (m, 2H), 8.25–8.14 (m, 1H), 7.43–7.27 (m, 3H), 7.27–7.12 (m, 3H), 7.07 (d, J = 6.2 Hz, 1H), 3.97 (s, 3H), 2.22 (d, J = 6.6 Hz, 3H). ^{13}C NMR (101 MHz, DMSO- d_6) δ 165.03, 163.24, 160.81, 149.45, 148.18, 146.10, 145.68, 141.37, 137.89, 136.66, 133.16, 131.42, 128.74, 128.47, 128.38, 121.78, 116.59, 116.37, 115.92, 115.62, 108.76, 60.04, 53.88, 23.49. ESI-MS m/z : 400.2 [M + H]⁺.

4.1.41. (*S*)-1-(1-(4-Fluorophenyl)ethyl)-8-(4-methoxyphenyl)-1*H*-[1,2,3]triazolo[4,5-*c*]quinolone (**14**). The title compound was prepared from **8e** (50 mg, 135 μmol) and commercially available (4-methoxyphenyl)boronic acid (21 mg, 135 μmol) using the procedure described for compound **1** in 89% yield as an off-white powder. ^1H NMR (400 MHz, CDCl_3) δ 9.58 (s, 1H), 8.38 (s, 1H), 8.25 (d, J = 8.6 Hz, 1H), 8.11 (d, J = 8.6 Hz, 1H), 7.68 (d, J = 8.4 Hz, 2H), 7.34–7.27 (m, 2H), 7.22 (t, J = 8.6 Hz, 2H), 7.14 (d, J = 8.4 Hz,

2H), 7.00 (q, $J = 6.4$ Hz, 1H), 3.86 (s, 3H), 2.20 (d, $J = 6.6$ Hz, 3H). ^{13}C NMR (101 MHz, DMSO- d_6) δ 163.26, 160.83, 160.03, 144.85, 144.44, 141.36, 139.40, 138.06, 133.11, 131.57, 131.12, 128.94, 128.58, 128.44, 128.36, 120.18, 116.61, 116.40, 115.73, 115.11, 60.12, 55.80, 23.59. ESI-MS m/z 399.1 [M + H]⁺.

4.1.42. (*S*)-4-(1-(4-Fluorophenyl)ethyl)-1*H*-[1,2,3]triazolo[4,5-*c*]quinolin-8-yl)benzamide (**15**). The title compound was prepared from **8e** (48 mg, 129 μmol) and commercially available (4-carbamoylphenyl)boronic acid (21 mg, 129 μmol) using the procedure described for compound **1** in 88% yield as a yellow powder. ^1H NMR (400 MHz, DMSO- d_6) δ 9.64 (s, 1H), 8.50 (d, $J = 1.7$ Hz, 1H), 8.32 (d, $J = 8.7$ Hz, 1H), 8.21 (dd, $J = 8.7$, 1.9 Hz, 1H), 8.12 (s, 1H), 8.09 (d, $J = 8.4$ Hz, 2H), 7.81 (d, $J = 8.4$ Hz, 2H), 7.49 (s, 1H), 7.36–7.28 (m, 2H), 7.22 (t, $J = 8.8$ Hz, 2H), 7.04 (q, $J = 6.7$ Hz, 1H), 2.22 (d, $J = 6.7$ Hz, 3H). ^{13}C NMR (101 MHz, DMSO- d_6) δ 167.89, 163.27, 160.84, 145.58, 145.06, 141.87, 141.39, 138.75, 137.99, 134.21, 133.18, 131.29, 128.99, 128.81, 128.44, 128.36, 127.58, 121.47, 116.61, 116.39, 115.69, 60.13, 23.60. ESI-MS m/z 412.2 [M + H]⁺.

4.1.43. (*S*)-4-(1-(4-Fluorophenyl)ethyl)-1*H*-[1,2,3]triazolo[4,5-*c*]quinolin-8-yl)morpholine (**16**). Compound **8e** (50 mg, 135 μmol , 1 equiv), morpholine (117 mg, 1.35 mmol, 10 equiv), Pd₂(dba)₃ (12 mg, 13.5 μmol , 0.1 equiv), X-Phos (13 mg, 27 μmol , 0.2 equiv), and K₂CO₃ (56 mg, 405 μmol , 3 equiv) were suspended in *t*-BuOH. Under a nitrogen atmosphere, the mixture was stirred at 100 °C overnight. The solvent was evaporated to dryness under reduced pressure to give the crude product, which was purified by flash column chromatography to yield the desired product as white powder (42.3 mg, 83% yield). ^1H NMR (400 MHz, DMSO- d_6) δ 9.33 (s, 1H), 8.02 (d, $J = 9.2$ Hz, 1H), 7.56 (d, $J = 9.2$ Hz, 1H), 7.41–7.31 (m, 3H), 7.27 (t, $J = 7.2$ Hz, 1H), 7.17 (d, $J = 7.6$ Hz, 2H), 6.83 (q, $J = 6.4$ Hz, 1H), 3.78 (t, $J = 4.6$ Hz, 4H), 3.31–3.21 (m, 2H), 3.17–3.06 (m, 2H), 2.18 (d, $J = 6.7$ Hz, 3H). ^{13}C NMR (101 MHz, DMSO- d_6) δ 163.25, 160.82, 150.13, 141.47, 141.33, 139.63, 138.31, 132.60, 131.27, 128.24, 128.15, 119.83, 116.58, 116.36, 104.95, 66.37, 60.03, 48.41, 23.67. ESI-MS m/z : 378.1 [M + H]⁺.

4.1.44. (*S*)-8-(4-Fluoro-3-methylphenyl)-1-(1-(4-fluorophenyl)ethyl)-1*H*-[1,2,3]triazolo[4,5-*c*]quinolone (**17**). The title compound was prepared from **8e** (50 mg, 135 μmol) and commercially available (4-fluoro-3-methylphenyl)boronic acid (21 mg, 135 μmol) using the procedure described for compound **1** in 92% yield as a white powder. ^1H NMR (400 MHz, CDCl₃) δ 9.59 (s, 1H), 8.34 (d, $J = 8.6$ Hz, 1H), 8.10 (d, $J = 1.8$ Hz, 1H), 7.92 (dd, $J = 8.6$, 2.0 Hz, 1H), 7.26–7.18 (m, 3H), 7.14 (t, $J = 8.8$ Hz, 1H), 7.11–7.04 (m, 2H), 6.46 (q, $J = 6.9$ Hz, 1H), 2.40 (d, $J = 1.8$ Hz, 3H), 2.32 (d, $J = 7.0$ Hz, 3H). ^{13}C NMR (101 MHz, DMSO- d_6) δ 163.24, 162.59, 160.81, 160.15, 145.24, 144.71, 141.38, 138.75, 138.06, 138.03, 135.45, 135.42, 133.15, 131.15, 130.99, 130.93, 128.82, 128.36, 128.28, 127.09, 127.01, 125.57, 125.39, 120.90, 116.62, 116.40, 116.23, 116.01, 115.64, 60.12, 23.61, 14.81, 14.78. ESI-MS m/z 401.0 [M + H]⁺.

4.1.45. (*S*)-4-(1-(4-Fluorophenyl)ethyl)-1*H*-[1,2,3]triazolo[4,5-*c*]quinolin-8-yl)benzonitrile (**18**). The title compound was prepared from **8e** (50 mg, 135 μmol) and commercially available (4-cyanophenyl)boronic acid (20 mg, 135 μmol) using the procedure described for compound **1** in 91% yield as an off-white powder. ^1H NMR (400 MHz, DMSO- d_6) δ 9.66 (s, 1H), 8.53 (d, $J = 1.8$ Hz, 1H), 8.34 (d, $J = 8.7$ Hz, 1H), 8.22 (dd, $J = 8.7$, 2.0 Hz, 1H), 8.07 (d, $J = 8.5$ Hz, 2H), 7.96 (d, $J = 8.5$ Hz, 2H), 7.35–7.27 (m, 2H), 7.21 (t, $J = 9.2$ Hz, 2H), 7.04 (q, $J = 6.7$ Hz, 1H), 2.20 (d, $J = 6.8$ Hz, 3H). ESI-MS m/z 394.1 [M + H]⁺.

4.1.46. (*S*)-1-(1-(4-Fluorophenyl)ethyl)-8-(pyridin-3-yl)-1*H*-[1,2,3]triazolo[4,5-*c*]quinolone (**19**). The title compound was prepared from **8e** (50 mg, 135 μmol) and commercially available pyridin-3-ylboronic acid (17 mg, 135 μmol) using the procedure described for compound **1** in 90% yield as a white powder. ^1H NMR (400 MHz, DMSO- d_6) δ 9.65 (s, 1H), 8.99 (d, $J = 2.4$ Hz, 1H), 8.68 (dd, $J = 4.8$, 1.5 Hz, 1H), 8.55 (d, $J = 1.6$ Hz, 1H), 8.34 (d, $J = 8.6$ Hz, 1H), 8.25–8.12 (m, 2H), 7.62 (dd, $J = 7.9$, 4.8 Hz, 1H), 7.36–7.27 (m, 2H), 7.24–7.14 (m, 2H), 7.08 (q, $J = 6.7$ Hz, 1H), 2.21 (d, $J = 6.8$ Hz, 3H). ^{13}C NMR (101 MHz, DMSO- d_6) δ 162.74, 160.31, 149.13, 148.16, 145.21, 144.59, 140.84, 137.44, 137.41, 136.20, 134.71, 134.35, 132.59, 130.98, 128.49,

127.99, 127.91, 123.99, 120.87, 116.03, 115.82, 115.25, 59.46, 22.98. ESI-MS m/z 370.1 [M + H]⁺.

4.1.47. (*S*)-1-(1-(4-Fluorophenyl)ethyl)-8-(1-methyl-1*H*-pyrazol-4-yl)-1*H*-[1,2,3]triazolo[4,5-*c*]quinolone (**20**). The title compound was prepared from **8e** (100 mg, 269 μmol) and commercially available (1-methyl-1*H*-pyrazol-4-yl)boronic acid (56 mg, 269 μmol) using the procedure described for compound **1** in 83% yield as an off-white powder. ^1H NMR (400 MHz, DMSO- d_6) δ 9.51 (s, 1H), 8.35 (s, 2H), 8.18 (d, $J = 8.7$ Hz, 1H), 8.08 (s, 1H), 8.05 (d, $J = 8.7$ Hz, 1H), 7.34 (dd, $J = 8.7$, 5.4 Hz, 2H), 7.18 (t, $J = 8.8$ Hz, 2H), 7.01 (q, $J = 6.7$ Hz, 1H), 3.95 (s, 3H), 2.22 (d, $J = 6.8$ Hz, 3H). ^{13}C NMR (101 MHz, DMSO- d_6) δ 163.20, 160.77, 144.19, 144.00, 141.34, 138.01, 137.15, 132.84, 132.55, 131.21, 129.26, 128.45, 128.37, 127.59, 121.37, 117.88, 116.51, 116.30, 115.93, 59.92, 39.34, 23.53. ESI-MS m/z 373.2 [M + H]⁺.

4.1.48. (*S*)-1-(5-(1-(1-(4-Fluorophenyl)ethyl)-1*H*-[1,2,3]triazolo[4,5-*c*]quinolin-8-yl)thiophen-2-yl)ethan-1-one (**21**). The title compound was prepared from **8e** (50 mg, 135 μmol) and commercially available (5-acetylthiophen-2-yl)boronic acid (23 mg, 135 μmol) using the procedure described for compound **1** in 74% yield as an off-white powder. ^1H NMR (400 MHz, DMSO- d_6) δ 9.64 (s, 1H), 8.50 (d, $J = 1.8$ Hz, 1H), 8.28 (d, $J = 8.7$ Hz, 1H), 8.22 (dd, $J = 8.7$, 2.0 Hz, 1H), 8.06 (d, $J = 4.0$ Hz, 1H), 7.85 (d, $J = 4.0$ Hz, 1H), 7.37–7.29 (m, 2H), 7.21–7.13 (m, 2H), 7.02 (q, $J = 6.6$ Hz, 1H), 2.61 (s, 3H), 2.22 (d, $J = 6.8$ Hz, 3H). ^{13}C NMR (101 MHz, DMSO- d_6) δ 191.17, 163.22, 160.79, 150.09, 145.86, 145.39, 144.44, 141.49, 137.75, 137.22, 135.61, 132.95, 132.15, 131.61, 128.43, 128.35, 127.84, 127.06, 120.27, 116.59, 116.38, 115.78, 60.18, 26.94, 23.54. ESI-MS m/z 417.1 [M + H]⁺.

4.1.49. (*S*)-4-(1-(1-(4-Fluorophenyl)ethyl)-1*H*-[1,2,3]triazolo[4,5-*c*]quinolin-8-yl)-3,5-dimethylisoxazole (**22**). The title compound was prepared from **8e** (50 mg, 135 μmol) and commercially available (3,5-dimethylisoxazol-4-yl)boronic acid (19 mg, 135 μmol) using the procedure described for compound **1** in 85% yield as an off-white powder. ^1H NMR (400 MHz, DMSO- d_6) δ 9.66 (s, 1H), 8.33 (d, $J = 8.6$ Hz, 1H), 8.28 (d, $J = 1.6$ Hz, 1H), 7.87 (dd, $J = 8.6$, 1.7 Hz, 1H), 7.26–7.14 (m, 4H), 6.93 (q, $J = 6.6$ Hz, 1H), 2.31 (s, 3H), 2.16 (d, $J = 6.8$ Hz, 3H), 2.14 (s, 3H). ^{13}C NMR (101 MHz, DMSO- d_6) δ 166.38, 163.25, 160.82, 158.71, 145.66, 144.68, 141.16, 137.54, 132.99, 131.23, 131.14, 129.97, 128.48, 128.40, 123.37, 116.41, 116.19, 115.93, 115.75, 59.78, 23.42, 11.68, 10.72. ESI-MS m/z 388.2 [M + H]⁺.

4.1.50. (*S*)-8-(Benzod[[1,3]dioxol-5-yl]-1-(1-(4-fluorophenyl)ethyl)-1*H*-[1,2,3]triazolo[4,5-*c*]quinolone (**23**). The title compound was prepared from **8e** (50 mg, 135 μmol) and commercially available benzo[[d][1,3]dioxol-5-yl boronic acid (22 mg, 135 μmol) using the procedure described for compound **1** in 83% yield as an off-white powder. ^1H NMR (400 MHz, DMSO- d_6) δ 9.59 (s, 1H), 8.36 (d, $J = 1.9$ Hz, 1H), 8.25 (d, $J = 8.7$ Hz, 1H), 8.09 (dd, $J = 8.7$, 2.0 Hz, 1H), 7.33 (d, $J = 1.8$ Hz, 1H), 7.32–7.26 (m, 2H), 7.24–7.15 (m, 3H), 7.12 (d, $J = 8.1$ Hz, 1H), 7.02 (q, $J = 6.7$ Hz, 1H), 6.14 (d, $J = 1.7$ Hz, 2H), 2.20 (d, $J = 6.8$ Hz, 3H). ^{13}C NMR (101 MHz, DMSO- d_6) δ 163.23, 160.80, 148.72, 148.02, 144.99, 144.57, 141.34, 139.46, 138.03, 138.00, 133.49, 133.10, 131.08, 128.83, 128.42, 128.34, 121.67, 120.45, 116.56, 116.34, 115.66, 109.35, 108.03, 101.90, 60.05, 23.54. ESI-MS m/z 413.1 [M + H]⁺.

4.1.51. (*S*)-8-(Benzofuran-5-yl)-1-(1-(4-fluorophenyl)ethyl)-1*H*-[1,2,3]triazolo[4,5-*c*]quinolone (**24**). The title compound was prepared from **8e** (100 mg, 269 μmol) and commercially available benzofuran-5-ylboronic acid (66 mg, 269 μmol) using the procedure described for compound **1** in 86% yield as an off-white powder. ^1H NMR (400 MHz, DMSO- d_6) δ 9.61 (s, 1H), 8.46 (d, $J = 1.8$ Hz, 1H), 8.30 (d, $J = 8.7$ Hz, 1H), 8.18 (dd, $J = 8.7$, 2.0 Hz, 1H), 8.12 (d, $J = 2.2$ Hz, 1H), 7.93 (d, $J = 1.7$ Hz, 1H), 7.80 (d, $J = 8.6$ Hz, 1H), 7.66 (dd, $J = 8.6$, 1.9 Hz, 1H), 7.36–7.28 (m, 2H), 7.28–7.20 (m, 2H), 7.13 (dd, $J = 2.2$, 0.9 Hz, 1H), 7.02 (q, $J = 6.7$ Hz, 1H), 2.21 (d, $J = 6.8$ Hz, 3H). ^{13}C NMR (101 MHz, DMSO- d_6) δ 163.30, 160.87, 154.82, 147.55, 145.08, 144.77, 144.61, 141.39, 140.15, 138.06, 134.64, 133.16, 131.15, 129.28, 128.57, 128.46, 128.38, 124.51, 121.24, 120.60, 116.65, 116.43, 115.71, 112.36, 107.56, 60.16, 23.57. ESI-MS m/z 409.0 [M + H]⁺.

4.1.52. (*S*)-(–)-5-(1-(1-(4-Fluorophenyl)ethyl)-1*H*-[1,2,3]triazolo[4,5-*c*]quinolin-8-yl)benzo[d]oxazole (**25**). The title compound was

prepared from **8e** (200 mg, 539 μmol) and self-prepared compound **28** (132 mg, 539 μmol) using the procedure described for compound **1** in 86% yield as a white powder, 99.1% HPLC purity; $[\alpha]_D^{25} = -238.32$ ($c = 0.107$, CH_3Cl , ee 100%). ^1H NMR (400 MHz, DMSO- d_6) δ 9.63 (s, 1H), 8.87 (s, 1H), 8.52 (d, $J = 1.4$ Hz, 1H), 8.32 (d, $J = 8.7$ Hz, 1H), 8.24 (dd, $J = 8.7, 1.7$ Hz, 1H), 8.18 (d, $J = 1.0$ Hz, 1H), 8.00 (d, $J = 8.3$ Hz, 1H), 7.78 (dd, $J = 8.3, 1.5$ Hz, 1H), 7.32 (dd, $J = 8.6, 5.4$ Hz, 2H), 7.20 (t, $J = 8.8$ Hz, 2H), 7.07 (q, $J = 6.6$ Hz, 1H), 2.22 (d, $J = 6.7$ Hz, 3H). ^{13}C NMR (101 MHz, DMSO- d_6) δ 163.26, 160.83, 155.66, 150.72, 145.46, 144.89, 141.39, 140.22, 139.24, 138.01, 137.36, 133.16, 131.29, 129.39, 128.48, 128.40, 124.84, 121.56, 121.02, 116.60, 116.39, 115.72, 110.50, 60.07, 23.56. ^{19}F NMR (376 MHz, TFA- d) δ -110.76. ESI-MS m/z 410.1 [M + H] $^+$. HRMS m/z (ESI) calcd for $\text{C}_{24}\text{H}_{17}\text{FN}_5\text{O}$ [M + H] $^+$ 410.1412, found 410.1410. HPLC purity analysis (mobile phase: $\text{H}_2\text{O}/\text{MeOH} = 25/75$, flow rate = 1.0 mL/min, $\lambda = 255.9$ nm, $t_R = 7.05$ min). Chiral HPLC analysis (mobile phase: 2-propanol/n-hexane = 30/70, flow rate = 1.0 mL/min, $\lambda = 255.9$ nm, $t_R = 40.50$ min).

4.1.53. 5-Bromobenzo[d]oxazole (27). 2-Amino-4-bromophenol (**26**, 2 g, 10.64 mmol) was added to triethyl orthoformate (30 mL) under a nitrogen atmosphere. The resulting mixture was refluxed for 8 h and monitored by TLC. After cooling to rt, triethyl orthoformate was removed under reduced pressure at 80 °C, and the residue was purified by column chromatography to yield the desired products as a white solid (1.89 g, 90% yield). ^1H NMR (400 MHz, DMSO- d_6) δ 8.82 (s, 1H), 8.07 (d, $J = 1.9$ Hz, 1H), 7.79 (d, $J = 8.7$ Hz, 1H), 7.62 (dd, $J = 8.7, 2.0$ Hz, 1H).

4.1.54. 5-(4,4,5,5-Tetramethyl-1,3,2-dioxaborolan-2-yl)benzo[d]oxazole (28). To a suspension of **27** (1 g, 5.05 mmol, 1 equiv), bis(pinacolato)diboron (1.54 g, 6.06 mmol, 1.2 equiv) and potassium acetate (1.49 g, 15.15 mmol, 3 equiv) in 1,4-dioxane, Pd(dppf)Cl₂ (184.76 mg, 0.25 mmol, 0.05 equiv) was added, and the mixture was stirred at 100 °C under a nitrogen atmosphere for 8 h. After cooling to rt, the solvent was evaporated to dryness under reduced pressure to obtain the crude product, which was purified by flash column chromatography to yield the desired product as an off-white powder (1.03 g, 83% yield). ^1H NMR (400 MHz, DMSO- d_6) δ 8.80 (s, 1H), 8.05 (s, 1H), 7.79 (d, $J = 8.2$ Hz, 1H), 7.76 (d, $J = 8.2$ Hz, 1H), 1.33 (s, 12H). ^{13}C NMR (101 MHz, DMSO- d_6) δ 154.87, 152.05, 140.05, 132.20, 126.71, 125.29, 111.42, 84.33, 25.13. ESI-MS m/z 246.1 [M + H] $^+$.

4.2. Pharmacological Experiments. **4.2.1. In Vitro Kinase Activity Assays.** CLK1 and DYRK1A kinase assays were conducted using the KinaseProfiler service of Eurofins Pharma Discovery Services UK Limited according to the protocols described below (for details on more kinases, see <http://www.eurofins.com/pharmadiscovery>). The concentration of ATP in each assay was 10 μM .

CLK1 (h) was incubated with 8 mM MOPS, pH 7.0, 0.2 mM EDTA, 1 mM sodium orthovanadate, 5 mM sodium β -glycerophosphate, 200 μM ERMRRPRKRQGSVRRRV, 10 mM magnesium acetate, and [γ -³³P]-ATP (specific activity and concentration as required). The reaction was initiated by addition of the Mg/ATP mixture. After incubation for 40 min at rt, the reaction was stopped by the addition of phosphoric acid at a concentration of 0.5%. A total of 10 μL of the reaction was then spotted onto a P30 filtermat, followed by washing four times for 4 min in 0.425% phosphoric acid and once in methanol prior to drying and scintillation counting.

DYRK1A (h) was incubated with 8 mM MOPS, pH 7.0, 0.2 mM EDTA, 50 μM RRRFRPASPLRGPPK, 10 mM magnesium acetate, and [γ -³³P]-ATP (specific activity and concentration as required). The reaction was initiated by addition of the Mg/ATP mixture. After incubation for 40 min at rt, the reaction was stopped by the addition of phosphoric acid at a concentration of 0.5%. A total of 10 μL of the reaction was then spotted onto a P30 filtermat, followed by washing four times for 4 min in 0.425% phosphoric acid and once in methanol prior to drying and scintillation counting.

4.2.2. Cell Culturing and Infection with Ad-mRFP-GFP-LC3. BNL CL.2 and SKOV-3 cells were maintained in Dulbecco's Modified Eagle's Medium and RPMI1640 media, respectively, both of which were supplemented with 10% fetal bovine serum. For adenovirus

infection, SKOV-3 cells were cultured with a half volume of culture media for 4 h that contained Ad-mRFP-GFP-LC3 (adenovirus coding tandem GFP-mRFP-LC3, Hanbio) and 5 $\mu\text{g}/\text{mL}$ polybrene. Then, the media was refreshed with culture media containing compound **25** or DMSO (0.1%). Cells were grown at 37 °C and 5% CO₂ in a humidified incubator.

4.2.3. Immunoblot Assays. Whole cell lysates were extracted with radioimmunoprecipitation assay (RIPA) lysis buffer (Beyotime Biotechnology) that contained phenylmethanesulfonyl fluoride (PMSF, Sigma), protease inhibitor cocktail (Sigma), and phosphatase inhibitor cocktail (Biotool.com). An equal amount of protein (10–25 $\mu\text{g}/\text{lane}$) was resolved by 12% or 10% sodium dodecyl sulfate polyacrylamide gel electrophoresis (SDS-PAGE) and transferred to polyvinylidene fluoride (PVDF) membranes (Millipore). The membranes were blocked with TBS-T blocking buffer (5% nonfat milk in TBS-T) for 2–3 h at rt and then probed with primary antibodies overnight at 4 °C. After three washes with TBS-T, the membranes were incubated with horseradish peroxidase-conjugated goat antimouse or antirabbit antibody (Cell Signaling Technology, 1:5000 dilution) for 1 h at 37 °C. After extensive washing with TBS-T, the membranes were preserved in TBS, and the immunoblots were visualized by ECL (Abbkine). Anti-LC3B (NOVUS, NB 600-1384, 1:1000 dilution) and anti-SQSTM1/p62 (Proteintech, 1:1000 dilution) antibodies were used to detect the level of autophagy and the degradation of autophagosomes, respectively, while anti-GAPDH antibodies (Cell Signaling Technology, 1:1000 dilution) were used to probe GAPDH as a control. Immunoblots were quantified using Adobe Photoshop software.

4.2.4. Immunofluorescence and Confocal Microscopy. For immunofluorescence, BNL CL.2 cells were treated with media containing **25** or DMSO for 24 h. Then, the cells were washed gently with PBS three times and fixed with 4% paraformaldehyde solution for 30 min. Fixed cells were washed with PBS and permeabilized with 0.5% Triton X-100 solution for 20 min. After three washes with PBS, cells were blocked by PBS blocking buffer (10% bovine albumin in PBS) for 30 min at rt. Then, the cells were incubated with anti-SR proteins antibody (mAb1H4G7, Invitrogen, 1:200 dilution) overnight at 4 °C to probe phosphorylated SR proteins. After three washes with PBS, in the absence of illumination, the cells were incubated with a secondary antibody (Cy3-conjugated AffiniPure goat antimouse IgG antibody, Proteintech, 1:50 dilution) for 30 min at 37 °C. Then, 0.5 $\mu\text{g}/\text{mL}$ 4',6-diamidino-2-phenylindole (DAPI) was used to visualize nuclei. Before examination, the cells were washed with PBS four times to remove residual DAPI. After treatment with **25** or DMSO, Ad-mRFP-GFP-LC3-infected cells were fixed with 4% paraformaldehyde solution before examination. The cells were viewed with an upright Leica confocal laser scanning microscope equipped with 40× and 63× oil immersion lenses.

4.2.5. In Vivo Study. Animal studies were conducted under the approval of the Experimental Animal Management Committee of Sichuan University. Male C57BL/6 mice were given either saline ($n = 3$, ip) or APAP (500 mg/kg) ($n = 15$, ip). To examine the hepatoprotective effect, mice were injected (ip) with **25** (30 mg/kg), **30** (30 mg/kg, positive control), rapamycin (30 mg/kg, positive control), or solvent (12.5% ethanol and 12.5% castor oil, 10 mL/kg), immediately followed by APAP (500 mg/kg) injection (ip). All mice were sacrificed 6 h later. Liver sections were examined by H&E staining, and the serum from the blood samples was used for ALT and AST activity tests.

4.3. CLK1/Inhibitor Co-crystallization and Structure Determination. **4.3.1. Plasmid Construction.** The coding sequence of human CLK1 (residues: 147–483) was cloned into the NdeI and XhoI restriction sites of pET22b (+) vector with a C-terminal His tag. The recombinant plasmid was successfully verified by DNA sequencing.

4.3.2. Protein Expression and Purification. The plasmid was transformed into *Escherichia coli* BL21 (DE3) competent cells. The transformant was grown at 37 °C until an OD₆₀₀ of 0.8 was reached and induced with 1 mM isopropyl- β -D-thiogalactoside (IPTG) at 18 °C overnight. The cells were resuspended in lysis buffer (50 mM

HEPES (pH 7.5), 500 mM NaCl, 5% glycerol, 50 mM L-glutamic acid, and 50 mM L-arginine) and lysed using a high pressure homogenizer at 4 °C. The insoluble debris was removed by centrifugation. The lysate was purified from the supernatants using Ni-NTA column chromatography. The eluted protein was further purified by size exclusion chromatography using a Superdex 200 Increase 10/300 GL (GE Healthcare) column in lysis buffer. The purified proteins were treated with lambda phosphatase overnight at 4 °C to remove phosphorylation and passed through the Superdexs 200 (10/300 GL) column again. The protein peak corresponding to homogeneous protein was collected. The quality of all purified samples was validated by SDS-PAGE analysis.

4.3.3. Crystallization and Data Collection. For co-crystallization, CLK1 protein was concentrated to 13 mg/mL and mixed with saturated X solution overnight in lysis buffer (50 mM HEPES (pH 7.5), 500 mM NaCl, 5% glycerol, 50 mM L-glutamic acid, and 50 mM L-arginine). The mixture was crystallized by the sitting-drop vapor diffusion method at 18 °C. Diffractable crystals of the complex were obtained in a condition consisting of 2% (v/v) PEG 200, 20% (v/v) tacsimate (pH 7.0), and 0.1 M HEPES (pH 9.0) and cryoprotected in the same precipitate solution containing 33% (v/v) glycerol. The diffraction data were collected at beamline BL17U1⁴¹ of Shanghai Synchrotron Radiation Facility (SSRF) using the synchrotron radiation. Data were then processed and scaled using the programs of HKL2000.⁴²

4.3.4. Structure Determination. The complex structure was solved by molecular replacement module of PHASER⁴³ from the CCP4 program suite,⁴⁴ and the CLK1/25 complex structure was solved with a previously reported CLK1 structure (PDB 2VAG) as the search model. The built structure model was further refined using REFMAC⁴⁵ and Phenix.⁴⁶ The atomic model was completed with Coot⁴⁷ and refined with phenix.refine.⁴⁶ The program of PROCHECK was used to assess the stereochemistry of the final model.

■ ASSOCIATED CONTENT

Supporting Information

The Supporting Information is available free of charge on the ACS Publications website at DOI: [10.1021/acs.jmedchem.7b00665](https://doi.org/10.1021/acs.jmedchem.7b00665).

Kinase inhibition profiles of **25** against a panel of 357 kinases; crystallographic data collection and refinement statistics; virtual screening led to the discovery of hit compound; dendrogram representation of the kinase selectivity profile of **25**; overview of X-ray cocrystal structure and a 2D ligand-interaction diagram of **25**; effects of **25** (20 and 100 nM) on the location and redistribution of SR proteins; detection of autophagy and autophagic flux induced by **25** (20 and 100 nM); in vitro effects of **18** on LC3; pharmacokinetic characteristics of **25**; IC₅₀ curves of **1**, **9e**, and **25** on CLK1 and DYRK1A; IC₅₀ curves of **25** on remaining kinases whose inhibitory rates were higher than 50% at 10 μM; pharmacokinetic assessments of **25**; synthesis and structure confirmation of **25R** (the enantiomer of **25**); copies of ¹H and ¹³C NMR spectra; copies of MS spectra; HPLC purity analysis for **25**; confirmation of enantiomeric purity of **25** (PDF)

Molecular formula strings (CSV)

Accession Codes

Coordinates and structure factors for structures of **25** have been deposited in the Protein Data Bank with the accession code of 5X8I. Authors will release the atomic coordinates and experimental data upon article publication.

■ AUTHOR INFORMATION

Corresponding Authors

*For S.-Y.Y.: phone, +86-28-85164063; fax, +86-28-85164060; E-mail, yangsy@scu.edu.cn.

*For G.-W.L.: E-mail, luguangwen2001@126.com.

ORCID

Sheng-Yong Yang: [0000-0001-5147-3746](http://orcid.org/0000-0001-5147-3746)

Author Contributions

[†]Q.-Z. S., G.-F. L. and L.-L. L. contributed equally to this work.

Notes

The authors declare no competing financial interest.

■ ACKNOWLEDGMENTS

We thank Prof. Stefan Knapp for providing us the plasmid of CLK1. This work was supported by the 973 Program (2013CB967204), the National Natural Science Foundation of China (81325021, 81473140, 81573349, and 81522026), and the Program for Changjiang Scholars and Innovative Research Team in University (IRT_17R78). Prof. Guangwen Lu is also in part supported by the National Key R&D Program of China (2016YFC1200300).

■ ABBREVIATIONS USED

CLK, cdc2-like kinase; DYRK, dual-specificity tyrosine-phosphorylation-regulated kinase; SR proteins, serine/arginine-rich proteins; LC3, microtubule-associated protein 1 light chain 3; mRFP, mammalian red fluorescent protein; Ad-mRFP-GFP-LC3, adenovirus coding tandem mRFP-GFP-LC3; DILI, drug-induced liver injury; H&E, hematoxylin and eosin; APAP, acetaminophen; ALT, alanine aminotransferase; AST, aspartate aminotransferase

■ REFERENCES

- (1) Janji, B.; Viry, E.; Moussay, E.; Paggetti, J.; Arakelian, T.; Mgrditchian, T.; Messai, Y.; Noman, M. Z.; Van Moer, K.; Hasmim, M.; Mami-Chouaib, F.; Berchem, G.; Chouaib, S. The multifaceted role of autophagy in tumor evasion from immune surveillance. *Oncotarget* **2016**, *7*, 17591–17607.
- (2) Lee, M. S. Role of islet beta cell autophagy in the pathogenesis of diabetes. *Trends Endocrinol. Metab.* **2014**, *25*, 620–627.
- (3) Riahi, Y.; Wikstrom, J. D.; Bachar-Wikstrom, E.; Polin, N.; Zucker, H.; Lee, M. S.; Quan, W.; Haataja, L.; Liu, M.; Arvan, P.; Cerasi, E.; Leibowitz, G. Autophagy is a major regulator of beta cell insulin homeostasis. *Diabetologia* **2016**, *59*, 1480–1491.
- (4) Frake, R. A.; Ricketts, T.; Menzies, F. M.; Rubinstein, D. C. Autophagy and neurodegeneration. *J. Clin. Invest.* **2015**, *125*, 65–74.
- (5) Menzies, F. M.; Fleming, A.; Rubinstein, D. C. Compromised autophagy and neurodegenerative diseases. *Nat. Rev. Neurosci.* **2015**, *16*, 345–357.
- (6) Ni, H. M.; Bockus, A.; Boggess, N.; Jaeschke, H.; Ding, W. X. Activation of autophagy protects against acetaminophen-induced hepatotoxicity. *Hepatology* **2012**, *55*, 222–232.
- (7) Ni, H. M.; Jaeschke, H.; Ding, W. X. Targeting autophagy for drug-induced hepatotoxicity. *Autophagy* **2012**, *8*, 709–710.
- (8) Morel, E.; Mehrpour, M.; Botti, J.; Dupont, N.; Hamai, A.; Nascimbeni, A. C.; Codogno, P. Autophagy: a druggable process. *Annu. Rev. Pharmacol. Toxicol.* **2017**, *57*, 375–398.
- (9) Gros, F.; Muller, S. Pharmacological regulators of autophagy and their link with modulators of lupus disease. *Br. J. Pharmacol.* **2014**, *171*, 4337–4359.
- (10) Levine, B.; Packer, M.; Codogno, P. Development of autophagy inducers in clinical medicine. *J. Clin. Invest.* **2015**, *125*, 14–24.

- (11) Breslin, E. M.; White, P. C.; Shore, A. M.; Clement, M.; Brennan, P. LY294002 and rapamycin co-operate to inhibit T-cell proliferation. *Br. J. Pharmacol.* **2005**, *144*, 791–800.
- (12) Coenen, J. J. A.; Koenen, H. J. P. M.; van Rijssen, E.; Hilbrands, L. B.; Joosten, I. Rapamycin, and not cyclosporin A, preserves the highly suppressive CD27⁺ subset of human CD4+CD25⁺ regulatory T cells. *Blood* **2006**, *107*, 1018–1023.
- (13) Houde, V. P.; Brule, S.; Festuccia, W. T.; Blanchard, P. G.; Bellmann, K.; Deshaies, Y.; Marette, A. Chronic rapamycin treatment causes glucose intolerance and hyperlipidemia by upregulating hepatic gluconeogenesis and impairing lipid deposition in adipose tissue. *Diabetes* **2010**, *59*, 1338–1348.
- (14) Lamming, D. W.; Ye, L.; Katajisto, P.; Goncalves, M. D.; Saitoh, M.; Stevens, D. M.; Davis, J. G.; Salmon, A. B.; Richardson, A.; Ahima, R. S.; Guertin, D. A.; Sabatini, D. M.; Baur, J. A. Rapamycin-induced insulin resistance is mediated by mTORC2 loss and uncoupled from longevity. *Science* **2012**, *335*, 1638–1643.
- (15) Fant, X.; Durieu, E.; Chicane, G.; Payrastre, B.; Sbrissa, D.; Shisheva, A.; Limanton, E.; Carreaux, F.; Bazureau, J. P.; Meijer, L. Cdc-like/dual-specificity tyrosine phosphorylation-regulated kinases inhibitor leucettine L41 induces mTOR-dependent autophagy: implication for Alzheimer's disease. *Mol. Pharmacol.* **2014**, *85*, 441–450.
- (16) Tahtouh, T.; Elkins, J. M.; Filippakopoulos, P.; Soundararajan, M.; Burgy, G.; Durieu, E.; Cochet, C.; Schmid, R. S.; Lo, D. C.; Delhommel, F.; Oberholzer, A. E.; Pearl, L. H.; Carreaux, F.; Bazureau, J.-P.; Knapp, S.; Meijer, L. Selectivity, cocrystal structures, and neuroprotective properties of leucettines, a family of protein kinase inhibitors derived from the marine sponge alkaloid leucettamine B. *J. Med. Chem.* **2012**, *55*, 9312–9330.
- (17) Debdab, M.; Carreaux, F.; Renault, S.; Soundararajan, M.; Fedorov, O.; Filippakopoulos, P.; Lozach, O.; Babault, L.; Tahtouh, T.; Baratte, B.; Ogawa, Y.; Hagiwara, M.; Eisenreich, A.; Rauch, U.; Knapp, S.; Meijer, L.; Bazureau, J.-P. Leucettines, a class of potent inhibitors of cdc2-like kinases and dual specificity, tyrosine phosphorylation regulated kinases derived from the marine sponge leucettamine B: modulation of alternative pre-RNA splicing. *J. Med. Chem.* **2011**, *54*, 4172–4186.
- (18) Giraud, F.; Alves, G.; Debiton, E.; Nauton, L.; Thery, V.; Durieu, E.; Ferandin, Y.; Lozach, O.; Meijer, L.; Anizon, F.; Pereira, E.; Moreau, P. Synthesis, protein kinase inhibitory potencies, and in vitro antiproliferative activities of meridianin derivatives. *J. Med. Chem.* **2011**, *54*, 4474–4489.
- (19) Fedorov, O.; Huber, K.; Eisenreich, A.; Filippakopoulos, P.; King, O.; Bullock, A. N.; Szklarczyk, D.; Jensen, L. J.; Fabbro, D.; Trappe, J.; Rauch, U.; Bracher, F.; Knapp, S. Specific CLK inhibitors from a novel chemotype for regulation of alternative splicing. *Chem. Biol.* **2011**, *18*, 67–76.
- (20) Esvan, Y. J.; Zeinyeh, W.; Boibessot, T.; Nauton, L.; Théry, V.; Knapp, S.; Chaikud, A.; Loaëc, N.; Meijer, L.; Anizon, F.; Giraud, F.; Moreau, P. Discovery of pyrido[3,4-g]quinazoline derivatives as CMGC family protein kinase inhibitors: design, synthesis, inhibitory potency and X-ray co-crystal structure. *Eur. J. Med. Chem.* **2016**, *118*, 170–177.
- (21) Coombs, T. C.; Tanega, C.; Shen, M.; Wang, J. L.; Auld, D. S.; Gerritz, S. W.; Schoenen, F. J.; Thomas, C. J.; Aubé, J. Small-molecule pyrimidine inhibitors of the cdc2-like (CLK) and dual specificity tyrosine phosphorylation-regulated (DYRK) kinases: development of chemical probe ML315. *Bioorg. Med. Chem. Lett.* **2013**, *23*, 3654–3661.
- (22) Drung, B.; Scholz, C.; Barbosa, V. A.; Nazari, A.; Sarragiotto, M. H.; Schmidt, B. Computational & experimental evaluation of the structure/activity relationship of β -carbolines as DYRK1A inhibitors. *Bioorg. Med. Chem. Lett.* **2014**, *24*, 4854–4860.
- (23) Rachdi, L.; Kariyawasam, D.; Guez, F.; Aiello, V.; Arbones, M. L.; Janel, N.; Delabar, J. M.; Polak, M.; Scharfmann, R. DYRK1A haploinsufficiency induces diabetes in mice through decreased pancreatic beta cell mass. *Diabetologia* **2014**, *57*, 960–969.
- (24) Fernandez-Martinez, P.; Zahonero, C.; Sanchez-Gomez, P. DYRK1A: the double-edged kinase as a protagonist in cell growth and tumorigenesis. *Mol. Cell. Oncol.* **2015**, *2*, e970048.
- (25) Muraki, M.; Ohkawara, B.; Hosoya, T.; Onogi, H.; Koizumi, J.; Koizumi, T.; Sumi, K.; Yomoda, J.; Murray, M. V.; Kimura, H.; Furuchi, K.; Shibuya, H.; Krainer, A. R.; Suzuki, M.; Hagiwara, M. Manipulation of alternative splicing by a newly developed inhibitor of CLKs. *J. Biol. Chem.* **2004**, *279*, 24246–24254.
- (26) Degorce, S. L.; Barlaam, B.; Cadogan, E.; Dishington, A.; Ducray, R.; Glossop, S. C.; Hassall, L. A.; Lach, F.; Lau, A.; McGuire, T. M.; Nowak, T.; Ouvry, G.; Pike, K. G.; Thomason, A. G. Discovery of novel 3-quinoline carboxamides as potent, selective, and orally bioavailable inhibitors of ataxia telangiectasia mutated (ATM) kinase. *J. Med. Chem.* **2016**, *59*, 6281–6292.
- (27) Glatthar, R.; Stojanovic, A.; Troxler, T.; Mattes, H.; Mobitz, H.; Beerli, R.; Blanz, J.; Gassmann, E.; Druckes, P.; Fendrich, G.; Gutmann, S.; Martiny-Baron, G.; Spence, F.; Hornfeld, J.; Peel, J. E.; Sparrer, H. Discovery of imidazoquinolines as a novel class of potent, selective, and in vivo efficacious cancer osaka thyroid (COT) kinase inhibitors. *J. Med. Chem.* **2016**, *59*, 7544–7560.
- (28) Haile, P. A.; Votta, B. J.; Marquis, R. W.; Bury, M. J.; Mehlmann, J. F.; Singhaus, R., Jr.; Charnley, A. K.; Lakdawala, A. S.; Convery, M. A.; Lipshutz, D. B.; Desai, B. M.; Swift, B.; Capriotti, C. A.; Berger, S. B.; Mahajan, M. K.; Reilly, M. A.; Rivera, E. J.; Sun, H. H.; Nagilla, R.; Beal, A. M.; Finger, J. N.; Cook, M. N.; King, B. W.; Ouellette, M. T.; Totoritis, R. D.; Pierdomenico, M.; Negroni, A.; Stronati, L.; Cucchiara, S.; Ziolkowski, B.; Vossenkämper, A.; MacDonald, T. T.; Gough, P. J.; Bertin, J.; Casillas, L. N. The identification and pharmacological characterization of 6-(tert-butylsulfonyl)-N-(5-fluoro-1H-indazol-3-yl)quinolin-4-amine (GSK583), a highly potent and selective inhibitor of RIP2 kinase. *J. Med. Chem.* **2016**, *59*, 4867–4880.
- (29) Jain, P.; Karthikeyan, C.; Moorthy, N. S.; Waiker, D. K.; Jain, A. K.; Trivedi, P. Human cdc2-like kinase 1 (CLK1): a novel target for Alzheimer's disease. *Curr. Drug Targets* **2014**, *15*, 539–550.
- (30) Colwill, K.; Pawson, T.; Andrews, B.; Prasad, J.; Manley, J. L.; Bell, J. C.; Duncan, P. I. The CLK/STY protein kinase phosphorylates SR splicing factors and regulates their intranuclear distribution. *EMBO J.* **1996**, *15*, 265–275.
- (31) Xie, Z.; Nair, U.; Klionsky, D. J. Atg8 controls phagophore expansion during autophagosome formation. *Mol. Biol. Cell* **2008**, *19*, 3290–3298.
- (32) Nakatogawa, H.; Ichimura, Y.; Ohsumi, Y. Atg8, a ubiquitin-like protein required for autophagosome formation, mediates membrane tethering and hemifusion. *Cell* **2007**, *130*, 165–178.
- (33) Kadokawa, M.; Karim, M. R. Cytosolic LC3 ratio as a quantitative index of macroautophagy. *Methods Enzymol.* **2009**, *452*, 199–213.
- (34) Karim, M. R.; Kanazawa, T.; Daigaku, Y.; Fujimura, S.; Miotto, G.; Kadokawa, M. Cytosolic LC3 ratio as a sensitive index of macroautophagy in isolated rat hepatocytes and H4-II-E cells. *Autophagy* **2007**, *3*, 553–560.
- (35) Mizushima, N.; Yoshimori, T.; Levine, B. Methods in mammalian autophagy research. *Cell* **2010**, *140*, 313–326.
- (36) Singh, K.; Sharma, A.; Mir, M. C.; Drazba, J. A.; Heston, W. D.; Magi-Galluzzi, C.; Hansel, D.; Rubin, B. P.; Klein, E. A.; Almasan, A. Autophagic flux determines cell death and survival in response to Apo2L/TRAIL (dulanermin). *Mol. Cancer* **2014**, *13*, 70.
- (37) Chen, M.; Borlak, J.; Tong, W. A model to predict severity of drug-induced liver injury in humans. *Hepatology* **2016**, *64*, 931–940.
- (38) Larson, A. M.; Polson, J.; Fontana, R. J.; Davern, T. J.; Lalani, E.; Hynan, L. S.; Reisch, J. S.; Schiott, F. V.; Ostapowicz, G.; Shakil, A. O.; Lee, W. M. Acetaminophen-induced acute liver failure: results of a United States multicenter, prospective study. *Hepatology* **2005**, *42*, 1364–1372.
- (39) Ni, H. M.; Williams, J. A.; Jaeschke, H.; Ding, W. X. Zonated induction of autophagy and mitochondrial spheroids limits acetaminophen-induced necrosis in the liver. *Redox Biol.* **2013**, *1*, 427–432.

- (40) Kheloufi, M.; Boulanger, C. M.; Durand, F.; Rautou, P. E. Liver autophagy in anorexia nervosa and acute liver injury. *BioMed Res. Int.* **2014**, *2014*, 701064.
- (41) Wang, Q. S.; Yu, F.; Huang, S.; Sun, B.; Zhang, K. H.; Liu, K.; Wang, Z. J.; Xu, C. Y.; Wang, S. S.; Yang, L. F.; Pan, Q. Y.; Li, L.; Zhou, H.; Cui, Y.; Xu, Q.; Thomas, E.; He, J. H. The macromolecular crystallography beamline of SSRF. *Nucl. Sci. Technol.* **2015**, *26*, 010102.
- (42) Otwinowski, Z.; Minor, W. Processing of X-ray diffraction data collected in oscillation mode. *Methods Enzymol.* **1997**, *276*, 307–326.
- (43) Read, R. J. Pushing the boundaries of molecular replacement with maximum likelihood. *Acta Crystallogr., Sect. D: Biol. Crystallogr.* **2001**, *57*, 1373–1382.
- (44) Collaborative, C. P.. The CCP4 suite: programs for protein crystallography. *Acta Crystallogr., Sect. D: Biol. Crystallogr.* **1994**, *50*, 760–763.
- (45) Murshudov, G. N.; Vagin, A. A.; Dodson, E. J. Refinement of macromolecular structures by the maximum-likelihood method. *Acta Crystallogr., Sect. D: Biol. Crystallogr.* **1997**, *53*, 240–255.
- (46) Adams, P. D.; Afonine, P. V.; Bunkóczki, G.; Chen, V. B.; Davis, I. W.; Echols, N.; Headd, J. J.; Hung, L.-W.; Kapral, G. J.; Grossesse-Kunstleve, R. W.; McCoy, A. J.; Moriarty, N. W.; Oeffner, R.; Read, R. J.; Richardson, D. C.; Richardson, J. S.; Terwilliger, T. C.; Zwart, P. H. PHENIX: a comprehensive Python-based system for macromolecular structure solution. *Acta Crystallogr., Sect. D: Biol. Crystallogr.* **2010**, *66*, 213–221.
- (47) Emsley, P.; Cowtan, K. Coot: model-building tools for molecular graphics. *Acta Crystallogr., Sect. D: Biol. Crystallogr.* **2004**, *60*, 2126–2132.